Imaging Neuroscience
an open access journal

Research Article

Brain functional connectivity predicts depression and anxiety during childhood and adolescence: A connectome-based predictive modeling approach

Francesca Morfini[a], Aaron Kucyi[b], Jiahe Zhang[a,c], Clemens C.C. Bauer[a,c,d], Paul A. Bloom[e,f], David Pagliaccio[e,f], Nicholas A. Hubbard[g], Isabelle M. Rosso[h,i], Anastasia Yendiki[j], Satrajit S. Ghosh[d], Diego A. Pizzagalli[h,i], John D.E. Gabrieli[d], Susan Whitfield-Gabrieli[a,c,d,j], Randy P. Auerbach[e,f]

[a]Department of Psychology, Northeastern University, Boston, MA, United States
[b]Department of Psychological and Brain Sciences, Drexel University, Philadelphia, PA, United States
[c]Center for Precision Psychiatry, Massachusetts General Hospital, Boston, MA, United States
[d]Department of Brain and Cognitive Sciences and McGovern Institute for Brain Research, Massachusetts Institute of Technology, Cambridge, MA, United States
[e]Department of Psychiatry, Columbia University, New York, NY, United States
[f]Division of Child and Adolescent Psychiatry, New York State Psychiatric Institute, Columbia University, New York, NY, United States
[g]Department of Psychology, University of Nebraska-Lincoln, Lincoln, NE, United States
[h]Center for Depression, Anxiety, and Stress Research, McLean Hospital, Belmont, MA, United States
[i]Department of Psychiatry, Harvard Medical School, Boston, MA, United States
[j]Athinoula A. Martinos Center for Biomedical Imaging, Massachusetts General Hospital, Charlestown, MA, United States

Corresponding Author: Francesca Morfini (f.morfini.work@gmail.com)

ABSTRACT

Identifying brain-based correlates of risk for future depression and anxiety severity in youth could improve prevention and treatment efforts. We tested whether connectome-based predictive modeling (CPM) based on resting-state functional connectivity (FC) at baseline: (a) predicts future depression and anxiety severity during childhood and (b) generalizes to adolescence. We used two independent, longitudinal datasets including children from the Adolescent Brain Cognitive Development (ABCD) study and adolescents from the Boston Adolescent Neuroimaging of Depression and Anxiety (BANDA). ABCD included a cohort of 11,875 children ages 9–11 years old, and BANDA enrolled 215 adolescents ages 14–17 years, of which ~70% reported a depressive or anxiety disorder. CPM with internal (within ABCD) and external validation (from ABCD to BANDA) used baseline whole-brain FC to predict depression and anxiety severity at a 1-year follow-up assessment. ABCD-derived functional connections, which we term "Symptoms Network", were validated within BANDA to test model applicability in adolescence, which is a peak period for the emergence of internalizing disorders. Participants with complete data were included from ABCD (n = 3,718, 52.9% girls, ages 10.0 ± 0.6) and BANDA (n = 150, 61.3% girls, ages 15.4 ± 0.9). In ABCD, we found that FC predicted 1-year follow-up symptoms severity ($\rho = 0.058$, $p = 0.040$), measured with the Child Behavior Checklist Anxious/Depressed subscale. External validation in BANDA indicated that the Symptoms Network predicted 1-year follow-up symptoms severity ($\rho = 0.222$, $p = 0.007$), measured with the Revised Child Depression and Anxiety Scale t-transformed total score. In both ABCD and BANDA, FC enhanced the prediction of future symptom severity beyond baseline clinical and demographic information (baseline severity, sex, and age), including when correcting for mean head motion. The ABCD-derived connections included contributions from somatomotor, attentional, and subcortical regions and were

Received: 9 March 2025 Revision: 16 August 2025 Accepted: 18 August 2025 Available Online: 25 August 2025

characterized by heterogeneous FC within adolescents, where the same region pairs were characterized by positive FC for some participants but by negative FC for others. In conclusion, FC may provide inroads for early identification of internalizing symptoms, which could inform preventative-intervention approaches prior to the emergence of affective disorders during a critical period of neuromaturation. However, the small effect sizes and heterogeneity in results underscore the challenges of employing brain-based biomarkers for clinical applications and emphasize the need for individualized approaches for understanding neurodevelopment and mental health.

Keywords: depression, anxiety, adolescence, functional connectivity, functional magnetic resonance imaging, longitudinal studies, machine learning

1. INTRODUCTION

Internalizing disorders, such as depression and anxiety, often co-occur throughout the course of childhood and adolescence (Auerbach et al., 2022) and are common and debilitating (Avenevoli et al., 2015; Essau, 2003, 2008; Kessler et al., 2005). Early onset of either anxiety or depression contributes to a more persistent (Batelaan et al., 2014; Beesdo et al., 2007; Kessler et al., 2012) and more complex psychiatric comorbidity during adulthood (Auerbach et al., 2016, 2018). Several initiatives—such as the Human Connectome Project (HCP) and the Adolescent Brain Cognitive Development (ABCD) study—provide large-scale and specialized neuroimaging datasets that can characterize neurodevelopmental vulnerability to internalizing disorders. These datasets, combined with recent advances in computational approaches, have enormous potential to augment our understanding of brain mechanisms related to depression and anxiety, which may improve our understanding of mental health as it develops in youth.

Functional connectivity (FC) during a resting state has identified promising neural correlates of depression and anxiety in functional magnetic resonance imaging (fMRI) studies. Depression is often characterized by altered FC, including hyperconnectivity of the default mode network (DMN), hyperconnectivity between the DMN and the frontoparietal network (FPN) often referred to as the central executive network (but see Uddin et al., 2023 for a discussion about network nomenclatures), and hypoconnectivity between FPN and dorsal attention network (DAN; Kaiser et al., 2015). With respect to anxiety disorders, research has observed within-network hypoconnectivity of the DMN, FPN, and salience network (or ventral attention network; VAN), DMN-FPN hypoconnectivity, and VAN-sensorimotor network (SMN) hypoconnectivity (Xu et al., 2019). However, these findings often rely on cross-sectional studies of adults (MacNamara et al., 2016) with fewer studies focusing on longitudinal characterization during development.

The availability of open-access, longitudinal datasets coupled with advancements in computational approaches (e.g., machine learning-based predictive models) has propelled research focused on FC linked to internalizing symptoms in youth (Gracia-Tabuenca et al., 2024; Toenders et al., 2019). Studies suggest that distributed connectivity patterns among frontal, parietal, and subcortical regions predict symptom severity in healthy or depressed-anxious children (Ho et al., 2022; Whitfield-Gabrieli et al., 2020), female adolescents with no history of depressive disorder (Jin et al., 2020), adolescents with internalizing disorders (Chahal, Kirshenbaum, et al., 2021; Chahal, Weissman, et al., 2021), and unaffected college students (He et al., 2021). Yet, to date, no study has investigated FC as a predictor of prospective symptom severity in children and then examined the generalizability to adolescents in independent data. This data-driven approach would enable the detection of neural patterns in children and extend them to adolescents, establishing whether mechanisms associated with mental health and neural development in childhood are also core to adolescence.

To address this gap, we identified FC predictors of internalizing symptoms over 1 year in predominantly healthy children and then tested whether these patterns predicted prospective anxious and depressive symptom severity in an independent sample of predominantly clinical (~70%) adolescents. Connectome-based predictive modeling (CPM; Shen et al., 2017), a data-driven machine-learning approach designed to investigate brain associations with continuous phenotypes, was applied in two independent, longitudinal, and clinically-heterogeneous datasets. The discovery dataset comprised a large community cohort from the ABCD study (Barch et al., 2018) of predominantly healthy children recruited during a peak time period for the emergence of anxiety disorders. The extension dataset included adolescents from the Boston Adolescent Neuroimaging of Depression and Anxiety (BANDA; Hubbard et al., 2020, 2024) HCP, a study that aimed to investigate depression and anxiety during a period of heightened vulnerability for internalizing disorders. Based on prior fMRI-FC studies investigating longitudinal predictors of depression and anxiety in youth (Ho et al., 2022; Whitfield-Gabrieli

et al., 2020, see also reviews; Macêdo et al., 2022; Toenders et al., 2019; van Tol et al., 2021), we expected that distributed FC patterns, including subcortical, occipital, and frontal regions, would predict internalizing symptoms across samples.

2. METHODS

2.1. Overview of datasets

Two independent longitudinal datasets were included (Fig. 1A). ABCD was utilized as the discovery dataset in CPM, and BANDA was leveraged to test the generalizability (for participant information, study design, symptom assessment, MRI data and MRI processing for ABCD, see Supplementary Appendices S1 and S2, and for BANDA Supplementary Appendices S3 and S4). For both datasets, each site received Institutional Review Board approval from their institution and written informed consent and assent were received by the guardian and participating children.

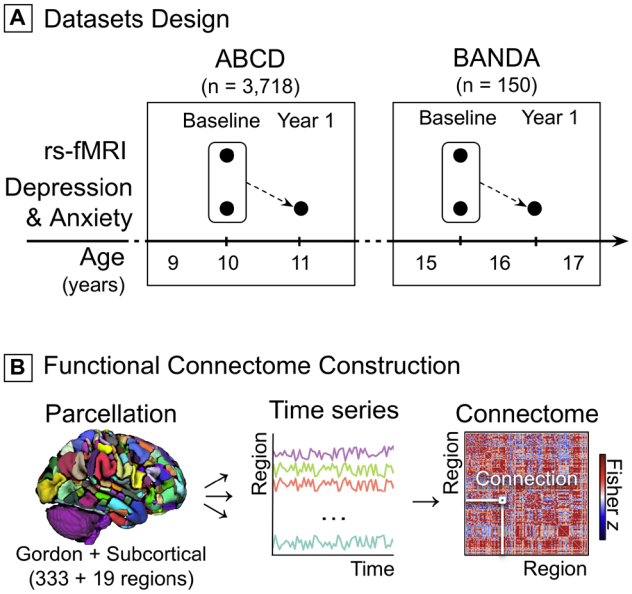

Fig. 1. Dataset design and connectomes construction. (A) Schematic representation of ABCD and BANDA study designs as a function of mean participant age at each study visit. Black dots indicate when rs-fMRI data and symptom severity reports were acquired. (B) rs-fMRI data for each participant were parcellated into 333 cortical (Gordon et al., 2016) and 19 subcortical (Fischl et al., 2002). The time series of each region was correlated with that of every other region to form a participant-specific connectome, wherein each region-to-region correlation represents a functional connection. Correlation coefficients were Fisher-z transformed. ABCD: Adolescent Brain Cognitive Development Study; BANDA: Boston Adolescent Neuroimaging of Depression and Anxiety; rs-fMRI: resting-state functional magnetic resonance imaging.

2.1.1. *ABCD: Discovery dataset*

ABCD is a publicly available, longitudinal, multi-site study in children (N = 11,875 from 21 sites) which recruited children from the community and assessed the presence of mental disorders but did not specifically recruit clinical populations. At baseline, participants were ages 9–11 years. Demographic and clinical information were obtained from the Annual Curated ABCD 4.0 Data Release (Barch et al., 2018). Resting-state fMRI (rs-fMRI) data (~20 minutes across four runs) were obtained from the ABCD-BIDS Community Collection 3165 (Feczko et al., 2021) and only included MRI data that passed the Data Analysis Imaging Center quality control (Chai et al., 2012). These data had been fully preprocessed and analyzed by the DCAN Lab via the ABCD-BIDS MRI pipeline (Feczko et al., 2021), which had been adapted from the HCP minimal preprocessing pipeline (Glasser et al., 2013). The child's depression and anxiety symptom severity was indicated via the Child Behavior Checklist (CBCL; Achenbach, 1991) Anxious/Depressed subscale *t*-transformed scores. The Anxious/Depressed subscale measures symptoms of anxiety and depression in children, such as excessive worrying, sadness, withdrawal, and nervousness, based on caregiver reports. It includes 13 items (range [0, 26]) with higher scores indicating greater symptom severity. See Supplementary Appendix S1 for further details.

We analyzed data collected between September 2016 and March 2020, which reflected the baseline and 1-year follow-up (Fig. 1A). The final sample included children (n = 3,718; Supplementary Fig. S1A) with available symptom severity reported at the baseline ($CBCL_{base}$) and 1-year follow-up ($CBCL_{y1}$), with no other family member scanned at another MRI site, and with at least 10 minutes of low-motion baseline rs-fMRI (FD < 0.25 mm).

2.1.2. *BANDA: Extension dataset*

BANDA is a publicly available, longitudinal, single-site dataset that investigated depression and anxiety in adolescents (Hubbard et al., 2020, 2024; Siless et al., 2020). Our research team collected these data from October 2016 to November 2021 and enrolled depressed-anxious and healthy adolescents (N = 215) ages 14–17 years. Data were obtained from the BANDA 1.1 Data Release (Hubbard et al., 2024). MRI (~23 minutes across four runs) data were pre-processed via the HCP minimal preprocessing pipeline (Glasser et al., 2013) and underwent fMRI quality control procedures (Morfini et al., 2023). Symptom severity was assessed via the self-report Revised Child Depression and Anxiety Scale (RCADS) *t*-transformed total scores (de Ross et al., 2002) which

assess overall levels of anxiety and depressive symptoms in youth, covering multiple specific disorders (e.g., generalized anxiety, social phobia, panic disorder, major depression) through self-report. See Supplementary Appendix S2 for further details. The final sample included adolescents (n = 150; Fig. 1A) with available symptom severity reported at the baseline ($RCADS_{base}$) and 1-year follow-up ($RCADS_{y1}$), and with low-motion rs-fMRI data at baseline (Supplementary Fig. S1B).

2.2. Functional connectomes construction

The degree to which different regions of the brain have synchronized activity can be summarized in a functional connectome, that is, a matrix of the correlations between the time series of every brain region to that of every other region. Connectomes for ABCD rs-fMRI data were constructed and released by the DCAN lab, with the brain parcellated into 352 regions (333 cortical from Gordon et al., 2016, and 19 subcortical from Fischl et al., 2002). For consistency, we adopted the same parcellation and method to build the connectomes for the BANDA adolescents (Fig. 1B), by calculating Fisher r-to-z-transformed Pearson's correlation coefficients between the time series of every region-to-region pair (i.e., one functional connection). This resulted in 61,776 unique functional connections, that is, [352 × (352-1)] / 2 unique connections, which were used as predictors in CPM.

2.3. ABCD Connectome-based predictive modeling analyses

CPM with leave-half-sites-out cross-validation (recommended for large sample sizes; Scheinost et al., 2019) consisted of five broad steps (Fig. 2A, B). *First*, all ABCD children acquired from a random selection of half of the ABCD sites were assigned to either a training or a testing set (Fig. 2A) and kept separate for all procedures of the same iteration. In light of the multi-site and nested nature of ABCD (which comprises members of the same family), splitting participants based on MRI site minimized the risk of information leakage between sets (Rosenblatt et al., 2024) and allowed to test for generalizability between different MRI sites within the ABCD dataset. *Second*, within the training set only, functional connections that correlated with $CBCL_{y1}$ (i.e., depression and anxiety severity at the 1-year follow-up) at a Spearman's rank correlation $p < 0.001$ were retained (Shen et al., 2017). We used Spearman's, rather than Pearson's, correlation to minimize the effect of outliers given that CBCL scores were positively skewed (Supplementary Fig. S2). *Third*, for each child, we calculated a composite FC measure (i.e., network strengths; Shen et al., 2017) as the sum of the *z* absolute values of the connections comprising the Network. Network strengths and $CBCL_{y1}$ in the training set were fit with a linear regression model. The fitted line was then used to generate $CBCL_{y1}$ predicted scores from network strengths in the testing set. Note that in the testing set pipeline, the $CBCL_{y1}$ observed scores were not used and the $CBCL_{y1}$ predicted scores were derived purely from network strengths (i.e., FC). *Fourth*, the networks' prediction performance was assessed in the testing set by computing a Spearman's partial correlation to compare observed versus predicted $CBCL_{y1}$, while correcting for symptom severity at baseline (i.e., $CBCL_{base}$), sex at birth, age, and mean head motion. These four steps were iterated 100 times generating a set of Spearman's ρ values which were averaged to represent the ability of the Network to predict $CBCL_{y1}$ within ABCD children. *Fifth*, as the training and testing sets were not independent across iterations resulting in an overestimation of the degrees of freedom in parametric statistics, the significance of the Network' prediction was assessed via nonparametric permutation testing (Fig. 2B). That is, the above four steps were permuted 1,000 times using randomly shuffled data (i.e., the connectome of a participant was used to predict the $CBCL_{y1}$ of another random participant) generating a set of plausible, yet not-observed, connectivity-to-symptom matches. The permuted ρ values generated represented an empirical null distribution against which we compared the prediction generated by the observed data. Specifically, the Network' prediction significance (p_{perm}) was defined as the proportion of permuted ρ values larger than the true ρ values (Shen et al., 2017). That is, the Network was considered to be significantly predictive only if less than 5% of the 1,000 predictions generated from shuffled data outperformed the prediction generated from observed data. This approach guards against the potential bias of using correlation in well-powered samples as it focuses on whether the observed effect is unusual, rather than simply significant, as compared to other scenarios which would have had a similar likelihood of being driven by sample size alone.

2.4. BANDA extension analyses

To test the generalizability of the predictions from the ABCD children to the prediction of prospective symptom severity in adolescents, we externally validated within BANDA (Shen et al., 2017) the ABCD-derived set of connections (Fig. 2C), which we refer to the "Symptoms Network" for brevity (but see Uddin et al., 2023 for some controversies regarding network nomenclature). The Symptoms Network, generated from all ABCD children, were used to generate composite measures of FC

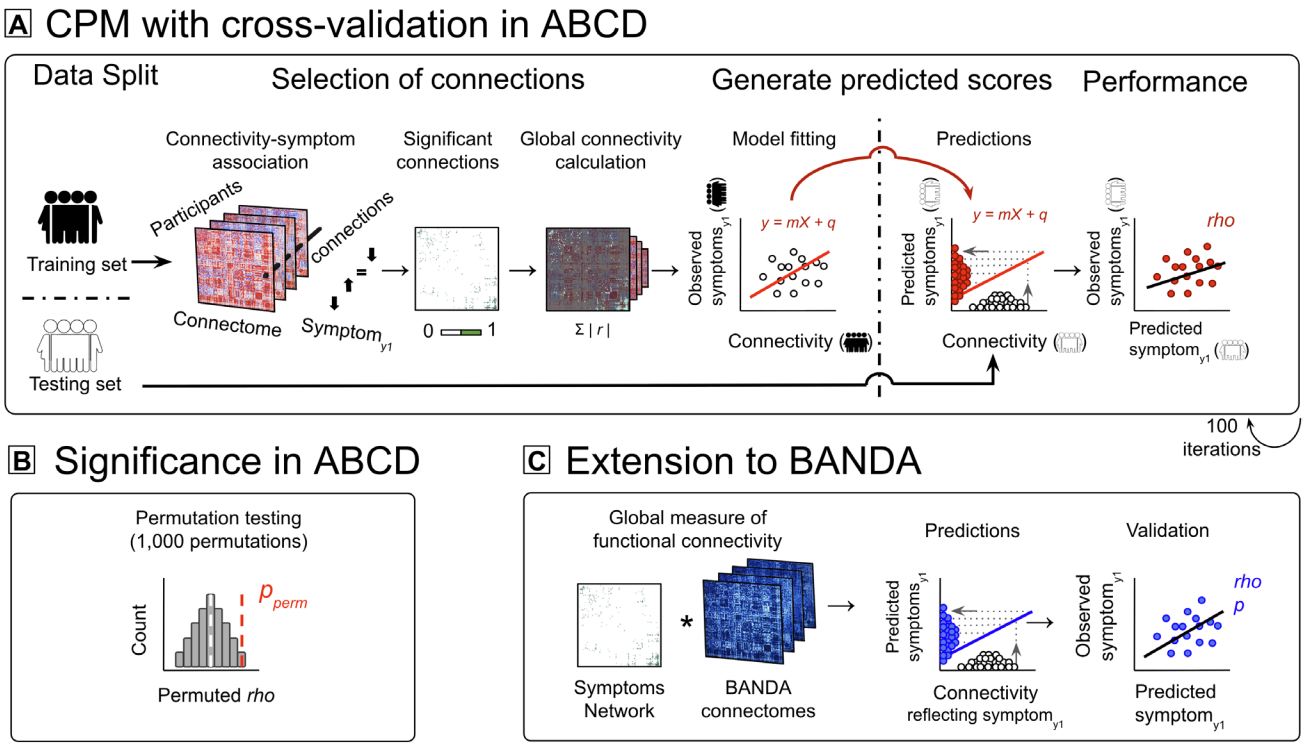

Fig. 2. Connectome-based predictive modeling in ABCD and external validation in BANDA. (A) In ABCD participants, CPM with 100 iterations and 1,000 permutations of leave-half-sites-out cross-validation used baseline whole-brain FC to predict symptom severity$_{y1}$, correcting for symptom severity$_{base}$, sex at birth, age, and mean head motion. The ABCD dataset was evenly split into a training and testing set. Within the training set, functional connections significantly correlated with symptom severity$_{y1}$ at $p < 0.001$ were retained. Network strengths were calculated as the sum of connection weights (i.e., absolute *z*-values). Network strengths and symptom severity$_{y1}$ were fit with a linear model in the testing set. The fitted line was used to generate predicted symptom severity$_{y1}$ scores from FC in the testing set. Networks' prediction performance was evaluated as the mean correlation between the observed and predicted symptom severity$_{y1}$ scores. (B) Network's prediction significance was assessed via nonparametric permutation testing with 1,000 permutations using randomly shuffled data. Significance (p_{perm}) was defined as the percentage of permuted ρ values larger than the ρ value generated from the observed data. (C) The ABCD-derived Network was externally validated in the independent BANDA dataset. Network strength scores were calculated for each BANDA adolescent and used to predict symptom severity$_{y1}$. Generalizability was defined as the Spearman's correlation between the network strengths and symptom severity$_{y1}$, correcting for symptom severity$_{base}$, sex at birth, age, and mean head motion. ABCD: Adolescent Brain Cognitive Development Study: BANDA, Boston Adolescent Neuroimaging of Depression and Anxiety; CPM: Connectome-Based Predictive Modeling; y1: 1-year follow-up assessment; FC: Functional Connectivity.

(i.e., network strengths) from the connectomes of each BANDA adolescent. These composite FC measures generated in BANDA were correlated with RCADS$_{y1}$, using Spearman's partial correlation (correcting for RCADS$_{base}$, sex at birth, age, and mean head motion), effectively testing whether FC predicted prospective depression and anxiety symptom severity in an independent cohort of adolescents mostly affected by depression and anxiety.

3. RESULTS

3.1. Participants

Demographic and clinical characteristics of the included ABCD children and BANDA adolescents are summarized in Figure 3 and Supplementary Tables S1–S3. Depression and anxiety severity—on average—remained stable in ABCD (CBCL$_{base}$ = 53.51 ± 6.02; CBCL$_{y1}$ = 53.48 ± 6.06) and decreased, that is, improved, in BANDA (RCADS$_{base}$ = 49.11 ± 15.28; RCADS$_{y1}$ = 44.62 ± 11.39) mostly driven by the depressed-anxious participants (RCADS$_{base}$ = 56.47 ± 14.26; RCADS$_{y1}$ = 49.07 ± 11.50) while the healthy group reported stable symptom severity between study visits (RCADS$_{base}$ = 36.04 ± 4.43; RCADS$_{y1}$ = 36.70 ± 5.25). Symptom severity scores reported at the baseline and at the 1-year follow-up assessments were correlated (Supplementary Fig. S2) in both ABCD children (r = 0.68, p = 0.001) and BANDA adolescents (r = 0.63, p = 0.001). Self-reported depression and anxiety severity (RCADS subscales) were strongly correlated in adolescents both at baseline (Pearson's two-sided r = 0.77 ± 0.11,

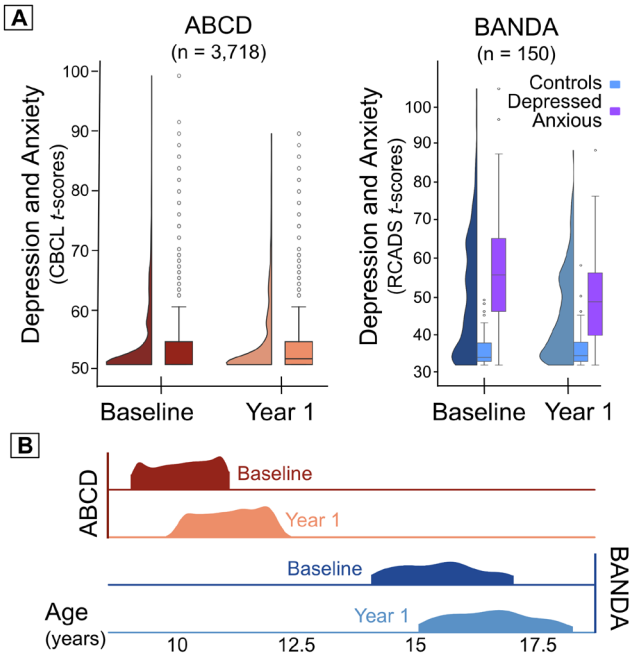

Fig. 3. Depression and anxiety severity and age distributions in ABCD children and BANDA adolescents. (A) Distributions of depression and anxiety severity scores for ABCD (left; $CBCL_{base}$ = 53.48 ± 6.06; $CBCL_{y1}$ = 53.51 ± 6.02) and for BANDA (right; $RCADS_{y1}$ = 49.11 ± 15.28; $RCADS_{base}$ = 44.62 ± 11.39). Controls and Depressed/Anxious group assignments in BANDA were based on a clinician evaluation of diagnoses as per the Diagnostic and Statistical Manual of Mental Disorders 5th edition (American Psychiatric Association, 2013) assessed with the Kiddie Schedule for Affective Disorders and Schizophrenia Present and Lifetime Version (Kaufman et al., 1997). (B) Age distributions at the time of study assessments in ABCD children (top, red distributions) and BANDA adolescents (bottom, blue distributions). ABCD: Adolescent Brain Cognitive Development Study; BANDA: Boston Adolescent Neuroimaging of Depression and Anxiety; CBCL: Child Behavior Checklist, Anxious/Depressed subscale *t*-transformed scores; RCADS: Revised Child Depression and Anxiety Scale, *t*-transformed total scores.

p-corrected $_{Bonferroni}$ < 0.0001, *r* range [0.56, 0.99]) and at the 1-year follow-up ((*r* = 0.73 ± 0.14, *p-corrected* $_{Bonferroni}$ < 0.0001, *r* range [0.42, 0.99]); Supplementary Table S4).

3.2. ABCD connectome-based predictive modeling

CPM revealed that baseline FC significantly predicted $CBCL_{y1}$ (correcting for $CBCL_{base}$, sex at birth, age, and mean head motion) in ABCD children (ρ = 0.058, p_{perm} = 0.040) reliably across multiple iterations of cross-validation and permutation testing. As expected, the distribution of shuffled-predicted correlations (Supplementary Fig. S3) was centered around ρ = 0 but could range between negative and positive values. A negative correlation in this context (i.e., between predicted and observed scores) would have represented cases where the predictions were inaccurate.

Sensitivity analyses suggest that these effects were robust to employing varied CPM analytical parameters, including different *p*-value thresholds for connection selection (0.05, 0.01, or 0.005) and for using raw rather than *t*-transformed severity scores severity scores (ρ = 0.062 ± 0.003 with range [0.058, 0.065]; *p* = 0.029 ± 0.011 with range [0.012, 0.038]). Additionally, there were no significant associations between in-scanner mean head motion (Supplementary Fig. S2), a confounding factor that artificially increases prediction performance if correlated with the predicted variable (Shen et al., 2017), and $CBCL_{base}$ (*r* = 0.01, *p* = 0.703) or $CBCL_{y1}$ (*r* = -0.02, *p* = 0.177).

These results were generated based on iterations of ABCD subsets of participants via the cross-validation approach and showed that results were reliable and robust regardless of the specific subset of individuals considered. Accordingly, we described and tested the performance of the connections that significantly correlate with $CBCL_{y1}$ scores (adjusted for $CBCL_{base}$, sex, age, and mean head motion) in all ABCD children. For brevity, we refer to this set of brain functional connections as the "Symptoms Network", which reflects results from the model: depression and anxiety *t*-transformed scores $_{y1}$ = depression and anxiety *t*-transformed scores $_{base}$ + sex $_{base}$ + age $_{base}$ + mean head motion $_{base}$ + functional connectivity $_{base}$.

3.3. Contextualizing the symptoms network

The Symptoms Network was characterized by connections distributed across the brain (Fig. 4), comprising 251 unique connections representing 0.41% of all possible connections.

To aid results interpretability, we grouped each cortical region to one of seven canonical brain networks (Yeo et al., 2011; see Supplementary Appendix S5 and Fig. S6) and counted the connections of all within- and between-canonical-network pairs. These counts were then normalized by the overall possible network-network connection counts (Greene et al., 2018; see Supplementary Appendix S6) which characterize the relative contribution of the canonical networks to the prediction of the future symptom severity ($CBCL_{y1}$ in children and $RCADS_{y1}$ in adolescents). Normalized count scores greater than 1 reflect canonical network pairs that are overrepresented in the prediction of symptom severity, that is, they contributed to prediction more than would be expected by chance.

The Symptoms Network (Fig. 5A) highlights three main patterns of (overrepresented) contributions involving sensory, attentional, and subcortical regions. The most

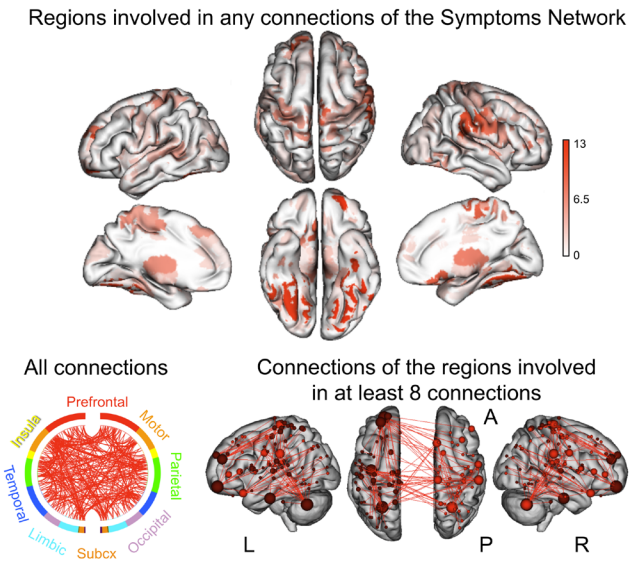

Fig. 4. Symptoms Network. CPM identified a predictive network in ABCD representing functional connections correlated with $CBCL_{y1}$ correcting for $CBCL_{base}$, sex, age, and mean head motion. The top panel reflects the distribution of the regions involved in at least one connection with another region in the Symptoms Network, color coded by absolute connection count. The chord plot (bottom left) depicts the spatial distribution of all identified connections based on anatomical macroscale lobe definition. The brain images (bottom right) depict the spatial distribution and degree (i.e., number of non-zero connections represented by the size of the node) of the Symptoms Network. For visualization purposes, only regions with degree ≥ 8 are displayed on the brain rendering images.

numerous connections and most widely distributed patterns involved the SMN, involving every combination of network-network pairs, including within-SMN, between SMN to all other cortical networks, and SMN-to-subcortical regions. Notably, the only non-represented contributions were from SMN-FPN. Furthermore, there were numerous contributions involving the VAN, including within-VAN, between VAN or DAN to other cortical networks, and VAN-to-subcortical regions. Lastly, predictions relied on numerous connections involving subcortical regions which were more sparsely connected to associative areas (DMN, FPN, and VAN) and subcortical to SMN. The most numerous contributions in the subcortical-SMN connections involved the thalamus and basal ganglia (caudate, putamen, and pallidum; Fig. 5A, bottom).

Similar patterns are highlighted by the overall absolute, rather than normalized, network-network connection counts (Supplementary Fig. S7).

To better describe the FC profiles of the Symptoms Network in adolescents, we grouped the connections of the Symptoms Network into connections that were either positively or negatively correlated with $RCADS_{y1}$ (representing brain-behavior associations at the group level). For each set of connections and network-to-network pair separately, we calculated the mean FC of each participant independently for the selected connections (representing FC profiles at the individual level). Figure 5B represents the within-participant FC distribution by network-to-network pairs, where each dot in the plot is the mean FC value of one participant.

The mean FC of the Symptoms Network was highly heterogeneous. In most network-to-network pairs, roughly half of the adolescents were characterized by positive FC and half by negative FC, that is, the participants' FC were distributed around a mean connectivity of zero (e.g., see the FC distribution of within-limbic, DMN-DAN, limbic-FPN, SMN-limbic, and subcortical-SMN among others in Fig. 5B). Virtually every network-to-network comprised both connections that were either positively or negatively correlated with future symptom severity–that is, most network-to-network pairs are included in both Figure 5B top and bottom plots (e.g., see within-VAN). Furthermore, results were mixed also with respect to the association with future symptom severity—wherein strong FC of a network-to-network pair was associated with worse or milder symptom severity depending on the specific connection. For example, within-SMN connections were characterized by positive FC among all included adolescents whether positive FC was correlated with worse (Fig. 5B, top) or with mild (Fig. 5B, bottom) symptom severity.

However, some networks were characterized by similar FC patterns. Within-network connections of VAN-VAN, SMN-SMN, and limbic-limbic consistently displayed stronger positive FC, indicating cohesive activity patterns within each canonical functional network. With respect to subcortical connections (Supplementary Fig. S8), mean FC profiles showed similar heterogeneity wherein connections were mostly characterized by positive FC and every network-network pair comprised both positive and negative connections. However, as compared to other subcortical-to-cortical connections, the pallidum (to SMN) and amygdala (to DMN and to DAN) FC values were less spread, suggesting higher concordance between participants.

3.4. Extension of the symptoms network from ABCD to BANDA

The Symptoms Network, generated from ABCD, significantly predicted $RCADS_{y1}$ in BANDA adolescents (Spearman's rank correlation ρ = 0.236, p = 0.004, mean absolute error [MAE] = 9.40, root mean square error [RMSE] = 14.54). Critically, the prediction held even after

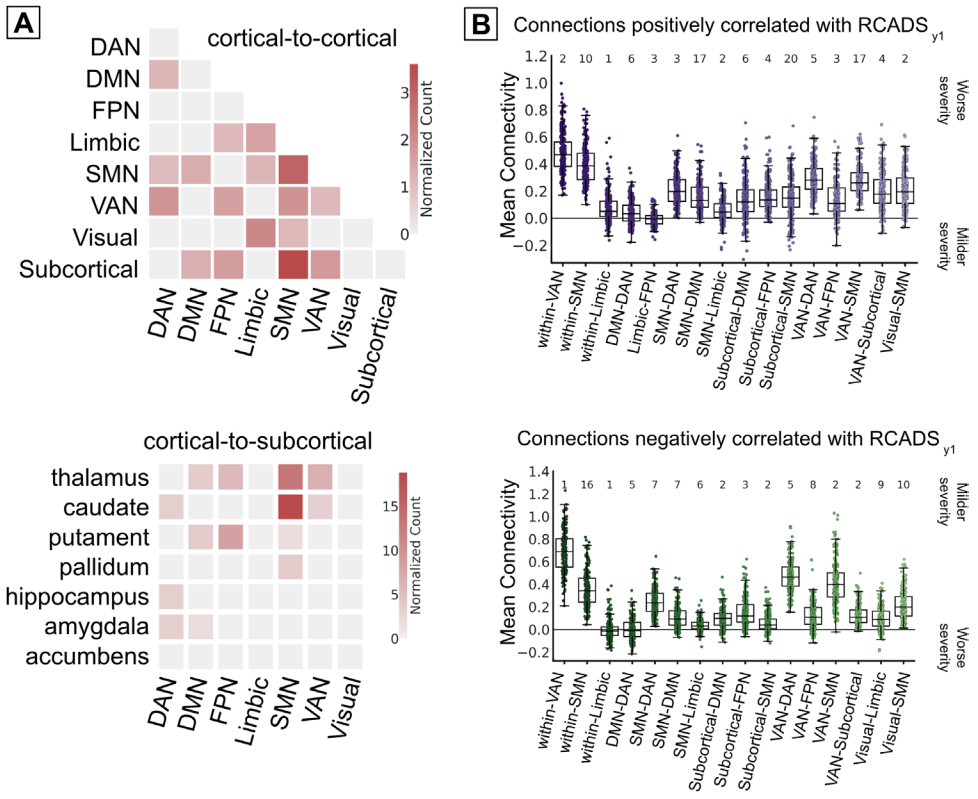

Fig. 5. Network functional connectivity profiles characterization. (A) Normalized connection counts of overrepresented canonical cortical-to-cortical and cortical-to-subcortical pairs of the Symptoms Network. (B) Boxplots represent the distribution of mean FC values among connections from overrepresented network-network pairs, calculated for each participant separately. For interpretation purposes, we report separately the mean FC of the connections that were positively (top, purple) or negatively (bottom, green) correlated with $RCADS_{y1}$. The numbers at the top of the graph represent the absolute connection counts of each network-network pair. For example, each value in the VAN-VAN distribution (panel B, purple) represents the mean FC of 10 connections for an individual participant. DAN: Dorsal Attention Network; DMN: Default Mode Network; FPN: Frontoparietal Network; SMN: Somatomotor Network; VAN: Ventral Attention Network.

partialling out the effect of $RCADS_{base}$, sex at birth, age, and mean head motion (Spearman's rank partial correlation ρ = 0.222, p = 0.007, MAE = 9.82, RMSE = 14.67; Supplementary Fig. S4).

3.5. Specificity of the symptoms network

We conducted specificity analysis for the Symptoms Network in both ABCD and BANDA datasets. In ABCD, specificity analyses (Supplementary Fig. S3) showed that the CBCL Anxious/Depressed subscale (i.e., the $CBCL_{y1}$) was the CBCL subscale (out of 20 subscales) with the strongest correlation to the network strengths (i.e., FC) defined by the Symptoms Network. Note, differently from how we evaluated the performance and significance of the Symptoms Network, Supplementary Figure S3 reports the results of Spearman's partial correlations generated on the full sample (n = 3,718) without employing cross-validation nor permutation testing. Thus, these are correlations and not predictions. As such, it was expected that the correlation (ρ = 0.198, Supplementary Fig. S3) would be inflated as compared to the predictions (ρ = 0.058), which were generated with a conservative approach.

In BANDA, specificity analyses revealed that $RCADS_{y1}$ were the scores that the Symptoms Network predicted best among other self-reported measures of other psychopathology, cognitive, and general demographic measures (Supplementary Fig. S4), acquired as part of the full protocol for the BANDA study (for further details see Supplementary Appendix S3 and Hubbard et al., 2024). This possibly suggests that the Symptoms Network was sensitive to internalizing symptoms rather than reflecting a general vulnerability to psychopathology or other demographic characteristics. Furthermore, in-scanner head mean motion was not correlated with $RCADS_{base}$ (r < 0.001, p = 0.987) but was negatively correlated with $RCADS_{y1}$ (r = -0.02, p = 0.014; Supplementary Fig. S4). Quality control plots (Morfini et al., 2023) showed no evident bias in the connectivity estimates of each adoles-

cent (Supplementary Fig. S5A) but suggested the presence of some residual effect of head motion at the group level (Supplementary Fig. S5B). Thus, the potential detrimental effect of motion-correlated FC was further minimized by adjusting all ABCD and BANDA analyses for mean head motion.

4. DISCUSSION

Recent research has advanced the neural characterization of internalizing disorders in youth, but no research has investigated the generalizability of neural correlates of prospective symptom severity between childhood and adolescence. Addressing this gap, a CPM approach used in the childhood cohort (ABCD) identified a set of connections, which we term "Symptoms Network", whose functional connectivity (FC) was related to individual differences in symptom severity at a 1-year follow-up. The Symptoms Network significantly predicted future symptom severity in children, correcting for baseline symptom severity, sex, age, and in-scanner mean head motion. Then, we demonstrated that symptom predictions derived from the Symptoms Network generalized to an independent sample of adolescents (BANDA) oversampled for internalizing disorders. Together, these results suggest that brain FC patterns associated with childhood depression and anxiety may persist during adolescence. Our results might also suggest that brain functional patterns associated with adolescent vulnerability to anxiety and depression may be identifiable earlier during childhood.

The Symptoms Network comprised distributed connections (Fig. 4), highlighting the contribution of multiple FC patterns, consistent with recent findings (Gracia-Tabuenca et al., 2024; He et al., 2021; Ho et al., 2022; Jin et al., 2020; Whitfield-Gabrieli et al., 2020). The contributing connections predominantly involved somatomotor, attention, and subcortical regions (Fig. 5), regions that have been previously investigated (largely by cross-sectional studies of affected adults) but that are overall less emphasized in the existing literature. Connections from the attentional and somatomotor networks might be indicative of heightened somatic awareness, hypersensitivity to bodily sensations even at rest, and states of ruminative or inward oriented attention, which often characterize anxious (Bouziane et al., 2022; MacNamara et al., 2016; Sylvester et al., 2013) and depressive conditions (Cui et al., 2024; Kaiser et al., 2015; Liu et al., 2019; Tse et al., 2024). Furthermore, numerous connections were found also within the SMN and between the SMN to frontal cortical networks (i.e., DMN, DAN, and VAN). The brain cortical development follows a sensorimotor-to-associative gradient, wherein sensory regions tend to mature earlier compared to associative areas (Baum et al., 2022; Chai et al., 2012; Gogtay et al., 2004; Sydnor et al., 2023). Our results might suggest that regions (i.e., SMN) which tend to reach within-network coherence earlier during the lifespan (Bethlehem et al., 2022; Gogtay et al., 2004) might already reflect certain signatures of vulnerability to internalizing disorders and may explain why these patterns can be identified as early as in childhood and even at rest.

Contrary to our hypotheses, predictive contributions in our model relied less than expected on the DMN, FPN, and other frontal or associative regions. These regions have been often linked to symptom severity in depression and anxiety via DMN hyperconnectivity or DMN-FPN dysregulation (Kaiser et al., 2015; Menon, 2011; Sheline et al., 2009) and are common targets of neuromodulatory interventions for depression (Mayberg et al., 2005; Siddiqi et al., 2020; Uddin et al., 2025; Zhang et al., 2023). Our results do not imply that the DMN, FPN, and other well-replicated findings did not contribute, nor are they unrelated to symptom severity or predictions in our model. Rather, we found that networks that undergo substantial reorganization during development (i.e., SMN and subcortical) may offer additional predictive value and may also be associated with future symptom severity. Furthermore, recent evidence suggests a key involvement in depression of the salience network (Lynch et al., 2024)—which overlaps with, but is not identical to, the FPN used here. Specifically, the salience network is expanded in depression, occupying a greater proportion of the cortex and encroaching regions that are assigned to adjacent networks in healthy controls. Our CPM approach selected connections regardless of network affiliation, yet our interpretation relied on a priori parcellation-based assignments. This may have assigned connections at the border of the FPN to adjacent networks instead, such as the VAN, which could potentially explain the importance of VAN-to-other network contribution to the prediction of future symptoms and the heterogeneity in FC profiles found within each set of connections. Lastly, as our model was trained on primarily healthy children, it may also have captured a distinct signature of future risk rather than signatures of active psychopathology. These findings suggest that risk and disorder expression may involve different circuit-level signatures, with implications for tailoring prevention interventions specifically more so than treatment.

Adolescents were characterized by substantial heterogeneity in their predictive FC profiles. Across most brain regions, mean FC values were widely-distributed among adolescents and centered around weak positive scores, in line with past findings (Goldstein-Piekarski et al., 2022; Kaiser et al., 2015; MacNamara et al., 2016),

with a minority of adolescents being characterized by negative values (Fig. 5B; Supplementary Fig. S8). Virtually all network-to-network pairs (Fig. 5; Supplementary Fig. S7) included some connections whose stronger positive FC predicted more severe symptoms and some connections whose stronger positive FC predicted milder symptom severity. This pattern indicates that—on average across individuals—all identified connections contributed to the predictive model. However, the relevance to the prediction of each connection varied for every participant: a given connection might be a "protective" (i.e., associated with symptom improvement), "risk" (i.e., associated with symptom worsening), or neutral factor (i.e., marked by weak or near-zero association with symptom change), depending on the individual's unique connectivity profile. This suggests that multiple, distinct neural mechanisms might contribute meaningfully to similar outcomes (Westlin et al., 2023), highlighting the potential shortcomings of uniform treatment approaches that do not account for individual differences. Such heterogeneity—where individuals with comparable symptom profiles may exhibit different neural correlates—ultimately underscores the need to develop interventions tailored to the individual and informed by each individual's specific underlying mechanisms (Taxali et al., 2021).

The Symptoms Network predictions generalized from childhood to adolescence and were specific to anxiety and depression at both age ranges (Supplementary Figs. S3 and S4). This suggests the presence of common mechanisms associated with the psychopathology of both anxiety and depression, and at both age ranges. Anxiety and depression often co-occur; however, anxiety tends to emerge earlier in childhood (Kessler et al., 2005) and is often associated with homotypic and heterotypic trajectories with depression in adolescence. These data support the presence of an overlap between anxious and depressive states in adolescents (self-reported anxiety and depression correlations: baseline $r = 0.822$, $p < 0.001$; 1-year follow-up $r = 0.806$, $p < 0.001$) and underscores the challenge of uncoupling them (Auerbach et al., 2022). Testing the temporal mechanisms between anxiety and depression was beyond the scope of this study, but the generalizability of the Symptoms Network's predictions from a community-based cohort (ABCD) to a more focused cohort oversampled for internalizing disorders (BANDA) could be taken as support for shared mechanisms underlying both anxiety and depression and highlights the importance of investigating the comorbidity between depression and anxiety.

Although both ABCD and BANDA are longitudinal observational studies, we observed a reduction in symptom severity between baseline and 1-year follow-up study visits in BANDA anxious-depressed participants, while ABCD and BANDA healthy participants reported consistently low and stable symptom levels. This reduction may reflect regression to the mean or natural recovery from more severe symptoms over time (Streiner, 2001). Our CPM model accounted for baseline symptom severity and included a healthy control group to mitigate such effects in predictive analyses (Yu & Chen, 2015), though they may still influence symptom distributions at individual timepoints. Given the episodic nature of depression, some participants may have been assessed during a symptom peak at baseline. Furthermore, informal or formal support may have contributed to symptom improvement. Importantly, this variability in symptom trajectories represents meaningful outcome patterns that predictive models must capture to provide added clinical value.

Nonetheless, the Symptoms Network predictions had modest effect sizes ($\rho = 0.058$ for children and $\rho = 0.222$ for adolescents), underscoring the challenge of translating neural correlates into clinical tools. The goal of the present study was not to identify a single, unified, and unique set of connections that underlie future risk of depression and anxiety, but rather to assess whether FC enclosed some information that represented an early sign of vulnerability to future psychopathology. Differently from other well-known descriptors of future risk of internalizing disorder–such as being female, young, and with a familial risk–FC can be considered a modifiable factor (Zhang et al., 2023) despite reliable configuration within individuals (Gordon et al., 2023) and with highly individualized topographic patterns (Finn et al., 2015). This study examined whether distributed patterns of FC associated with adolescent internalizing psychopathology could be identified in childhood–a time period that often precedes disorder onset. Our findings offer insights into the role of FC in mental health as it evolves throughout youth.

Our results suggest that FC improved symptom prediction. We took several analytical precautions to ensure the reliability, validity, generalizability, and specificity of our results. For reliability (Fig. 2A), we employed a leave-half-sites-out cross-validation technique within the ABCD cohort, as this approach is recommended for large samples (Poldrack et al., 2020; Scheinost et al., 2019) with a nested data structure (Rosenblatt et al., 2024). Since ABCD includes family members and multiple MRI sites, this ensured independence between splits of the cross-validation. We used permutation testing (Fig. 2B) to define results significance, reducing false positives linked with the large sample size of ABCD. For generalizability, we tested whether the ABCD-derived network could generate significant predictions in independent data from BANDA adolescents (Fig. 2C). To address skewed symptom scores (Fig. 3A), we used Spearman's rank

correlation and *t*-transformed scores for robust, interpretable results. Specificity was assessed by comparing the prediction for anxiety/depression severity with measures expected to be unrelated, in both children (Supplementary Fig. S3) and adolescents (Supplementary Fig. S4). We also controlled for baseline symptom severity, sex, age, and mean head motion, showing that our model detected effects beyond established predictors of future risk. Overall, this study afforded a novel framework that combines the advantages of large samples with those of specialized datasets. While large publicly available datasets are well powered to detect small heterogeneous effects, their broad scope limits the ability to detail specific phenomena of interest, afforded instead by usually smaller specialized datasets. By combining both approaches, results can capture community-wide effects while offering insights into targeted phenomena. Within this framework, the Symptoms Network represents a data-driven marker of early vulnerability–trained on mostly healthy children yet predictive in both healthy and clinically affected adolescents. Detecting signatures of psychopathology risk in mostly healthy individuals and validating them in individuals experiencing anxiety or depression poses a significant yet crucial challenge for mental health research. Achieving added predictive performance despite these factors is critical for advancing early identification and prevention strategies, highlighting the potential value for real-world applications of biological markers (Woo et al., 2017).

4.1. Limitations

There are several noteworthy limitations. First, the datasets were not the same age ranges, and thus, not a direct validation of the ABCD-derived Symptoms Network. However, applying cross-validation internally to a large sample, such as ABCD, allows training and testing on well-powered subsamples of ~1,860 children (Garavan et al., 2018), guarding against overfitting. Second, while we referred to 9–10 years-old participants from ABCD as children, these ages could also be considered late childhood or early adolescence. Third, CPM tested for linear effects over time; however, it is plausible that symptom development could be characterized by non-linear trends. Fourth, although including all the possible functional connections in our CPM approach is consistent with standard practice in the field (Kucyi et al., 2021; Shen et al., 2017; Taxali et al., 2021), this high-dimensional feature space may reduce model precision due to multicollinearity and individual variability. Although this comprehensive modeling strategy captures the full connectome and preserves potential predictive signals, it may also contribute to higher rate of false negative errors and underestimation of true effect sizes. Fifth, although the prediction effect sizes were modest, they are in line with those reported in prior studies employing similar methodologies (Marek et al., 2022). It is noteworthy that unlike most studies, which examine the associations between brain connectivity and concurrent symptoms, the Symptoms Network predictions were further penalized by the challenge of predicting future severity (rather than concurrent). This prediction was further constrained by statistical correction for baseline severity, which itself was strongly correlated with 1-year follow-up severity across participants (Supplementary Fig. S2). These factors underscore the robustness of the observed predictive patterns despite the small effect sizes. Furthermore, small shifts in the effect size have been shown to impact disproportionally more the extreme cases of a distribution (Carey et al., 2023). In the case of mental health, these would be the individuals suffering from depression and anxiety, for example. For those, even small effect sizes may be both meaningful and impactful, especially considering the compounded effects of early prevention or interventions over time.

5. CONCLUSIONS

CPM identified FC patterns that predicted future depression and anxiety severity across independent samples of children and adolescents. Distributed connectivity patterns of attentional, sensorimotor, and subcortical systems contributed to the prediction of symptom severity at a 1-year follow-up assessment, suggesting that brain FC may meaningfully contribute to informing future depression and anxiety severity. Accordingly, neural networks may provide targets for the development and testing of treatments for youth (e.g., real-time neurofeedback, transcranial magnetic stimulation). However, the modest effect sizes and heterogeneity of results, as found in our study and other prior work, highlights the challenges of translating brain-based correlates into clinical tools and suggests that such correlates may not apply uniformly across individuals. Ultimately, our results point to the potential value of employing personalized approaches tailored to individual neurobiological profiles in youth.

DATA AND CODE AVAILABILITY

Publicly available datasets were analyzed in this study which can be found in the National Institute of Mental Health Data Archive data including *Connectomes Related to Anxiety and Depression in Adolescents (BANDA)* collection #3037 and *DCAN Labs ABCD-BIDS Community Collection (ABCC)* #3165. Analysis code for the current

project can be found at https://github.com/fmorfini/publications/tree/main/CPM_ABCD_BANDA_predict_future_depression_anxiety

AUTHOR CONTRIBUTIONS

R.P.A., J.D.E.G., S.S.G., N.A.H., F.M., D.A.P., S.W.G, and A.Y. conceptualized the study; R.P.A., C.C.C.B., P.A.B., J.D.E.G., S.S.G., N.A.H., A.K., F.M., D.P., D.A.P., I.M.R., S.W.G., A.Y., and J.Z. acquired, analyzed, interpreted the data, drafted the draft, and provided critical revision of the manuscript. All authors approved the final manuscript and agreed to be accountable for all aspects of the work in ensuring that questions related to the accuracy or integrity of any part of the work are appropriately investigated and resolved.

DECLARATION OF COMPETING INTEREST

Over the past 3 years, Dr. Pizzagalli has received consulting fees from Albright Stonebridge Group, Boehringer Ingelheim, Circular Genomics, Compass Pathways, Engrail Therapeutics, Neumora Therapeutics (formerly BlackThorn Therapeutics), Neurocrine Biosciences, Neuroscience Software, Otsuka, and Takeda; he has received honoraria from the Psychonomic Society and the American Psychological Association (for editorial work) and from Alkermes; he has received research funding from the Brain and Behavior Research Foundation, the Dana Foundation, Millennium Pharmaceuticals, NIMH, and Wellcome Leap; he has received stock options from Compass Pathways, Engrail Therapeutics, Neumora Therapeutics, and Neuroscience Software. In the past 3 years, Dr. Auerbach has received consulting fees and equity from Get Sonar Inc. He also has received consulting fees from RPA Health Consulting, Inc. and Covington & Burling LLP, which is representing a social media company in litigation. He has received research funding from NIMH, the Morgan Stanley Alliance, the Tommy Fuss Fund, and the Bender-Fishbein Foundation. All views expressed are solely those of the authors. All other authors have no conflicts of interest or relevant disclosures.

ACKNOWLEDGMENTS

We thank Dr. Juliet Y. Davidow for her invaluable feedback. Data were provided in part by the Boston Adolescent Neuroimaging of Anxiety and Depression (BANDA) Consortium's Human Connectome Project, supported by U01MH108168 (J.D.E.G., S.W.G., S.S.G), R01MH119771 (R.P.A.), and R56MH121426 (S.W.G., A.Y., R.P.A.). In part, data were obtained from the Adolescent Brain Cognitive Development (ABCD) Study (https://abcdstudy.org), held in the NIMH Data Archive (NDA). The ABCD Study® is supported by the National Institutes of Health and additional federal partners under award numbers U01DA041048, U01DA050989, U01DA051016, U01DA041022, U01DA051018, U01DA051037, U01DA050987, U01DA041174, U01DA041106, U01DA041117, U01DA041028, U01DA041134, U01DA050988, U01DA051039, U01DA041156, U01DA041025, U01DA041120, U01DA051038, U01DA041148, U01DA041093, U01DA041089, U24DA041123, and U24DA041147. A full list of supporters is available at https://abcdstudy.org/federal-partners.html. A listing of participating sites and a complete listing of the study investigators can be found at https://abcdstudy.org/consortium_members. The content is solely the responsibility of the authors and does not necessarily represent the official views of the National Institutes of Health.

SUPPLEMENTARY MATERIALS

Supplementary material for this article is available with the online version here: https://doi.org/10.1162/IMAG.a.145.

REFERENCES

Achenbach, T. M. (1991). *Manual for the Child Behavior Checklist/4-18 and 1991 Profile*. Department of Psychiatry, University of Vermont. https://archive.org/details/manualforchildbe0000ache_g2r5/mode/2up

American Psychiatric Association. (2013). *Diagnostic and statistical manual of mental disorders: DSM-5™* (5th ed., pp. xliv, 947). American Psychiatric Publishing, Inc. https://doi.org/10.1176/appi.books.9780890425596

Auerbach, R. P., Alonso, J., Axinn, W. G., Cuijpers, P., Ebert, D. D., Green, J. G., Hwang, I., Kessler, R. C., Liu, H., Mortier, P., Nock, M. K., Pinder-Amaker, S., Sampson, N. A., Aguilar-Gaxiola, S., Al-Hamzawi, A., Andrade, L. H., Benjet, C., Caldas-de-Almeida, J. M., Demyttenaere, K., … Bruffaerts, R. (2016). Mental disorders among college students in the World Health Organization World Mental Health Surveys. *Psychological Medicine*, *46*(14), 2955–2970. https://doi.org/10.1017/S0033291716001665

Auerbach, R. P., Mortier, P., Bruffaerts, R., Alonso, J., Benjet, C., Cuijpers, P., Demyttenaere, K., Ebert, D. D., Green, J. G., Hasking, P., Murray, E., Nock, M. K., Pinder-Amaker, S., Sampson, N. A., Stein, D. J., Vilagut, G., Zaslavsky, A. M., Kessler, R. C., & WHO WMH-ICS Collaborators. (2018). WHO World Mental Health Surveys International College Student Project: Prevalence and distribution of mental disorders. *Journal of Abnormal Psychology*, *127*(7), 623–638. https://doi.org/10.1037/abn0000362

Auerbach, R. P., Pagliaccio, D., Hubbard, N. A., Frosch, I., Kremens, R., Cosby, E., Jones, R., Siless, V., Lo, N., Henin, A., Hofmann, S. G., Gabrieli, J. D. E., Yendiki, A., Whitfield-Gabrieli, S., & Pizzagalli, D. A. (2022). Reward-related neural circuitry in depressed and anxious adolescents: A Human Connectome Project. *Journal of the American Academy of Child & Adolescent Psychiatry*, *61*(2), 308–320. https://doi.org/10.1016/j.jaac.2021.04.014

Avenevoli, S., Swendsen, J., He, J.-P., Burstein, M., & Merikangas, K. R. (2015). Major Depression in the National Comorbidity Survey–Adolescent Supplement: Prevalence, correlates, and treatment. *Journal of the American Academy of Child & Adolescent Psychiatry*, *54*(1), 37. e2–44.e2. https://doi.org/10.1016/j.jaac.2014.10.010

Barch, D. M., Albaugh, M. D., Avenevoli, S., Chang, L., Clark, D. B., Glantz, M. D., Hudziak, J. J., Jernigan, T. L., Tapert, S. F., Yurgelun-Todd, D., Alia-Klein, N., Potter, A. S., Paulus, M. P., Prouty, D., Zucker, R. A., & Sher, K. J. (2018). Demographic, physical and mental health assessments in the adolescent brain and cognitive development study: Rationale and description. *Developmental Cognitive Neuroscience*, *32*, 55–66. https://doi.org/10.1016/j.dcn.2017.10.010

Batelaan, N. M., Rhebergen, D., Spinhoven, P., Balkom, A. J. van, & Penninx, B. W. J. H. (2014). Two-year course trajectories of anxiety disorders: Do DSM classifications matter? *The Journal of Clinical Psychiatry*, *75*(9), 3905. https://doi.org/10.4088/JCP.13m08837

Baum, G. L., Flournoy, J. C., Glasser, M. F., Harms, M. P., Mair, P., Sanders, A. F. P., Barch, D. M., Buckner, R. L., Bookheimer, S., Dapretto, M., Smith, S., Thomas, K. M., Yacoub, E., Essen, D. C. V., & Somerville, L. H. (2022). Graded variation in T1w/T2w ratio during adolescence: Measurement, caveats, and implications for development of cortical myelin. *Journal of Neuroscience*, *42*(29), 5681–5694. https://doi.org/10.1523/JNEUROSCI.2380-21.2022

Beesdo, K., Bittner, A., Pine, D. S., Stein, M. B., Höfler, M., Lieb, R., & Wittchen, H.-U. (2007). Incidence of social anxiety disorder and the consistent risk for secondary depression in the first three decades of life. *Archives of General Psychiatry*, *64*(8), 903–912. https://doi.org/10.1001/archpsyc.64.8.903

Bethlehem, R. A. I., Seidlitz, J., White, S. R., Vogel, J. W., Anderson, K. M., Adamson, C., Adler, S., Alexopoulos, G. S., Anagnostou, E., Areces-Gonzalez, A., Astle, D. E., Auyeung, B., Ayub, M., Bae, J., Ball, G., Baron-Cohen, S., Beare, R., Bedford, S. A., Benegal, V., …Alexander-Bloch, A. F. (2022). Brain charts for the human lifespan. *Nature*, *604*(7906), Article 7906. https://doi.org/10.1038/s41586-022-04554-y

Bouziane, I., Das, M., Friston, K. J., Caballero-Gaudes, C., & Ray, D. (2022). Enhanced top-down sensorimotor processing in somatic anxiety. *Translational Psychiatry*, *12*(1), 295. https://doi.org/10.1038/s41398-022-02061-2

Carey, E. G., Ridler, I., Ford, T. J., & Stringaris, A. (2023). Editorial perspective: When is a "small effect" actually large and impactful? *Journal of Child Psychology and Psychiatry, and Allied Disciplines*, *64*(11), 1643–1647. https://doi.org/10.1111/jcpp.13817

Chahal, R., Kirshenbaum, J. S., Miller, J. G., Ho, T. C., & Gotlib, I. H. (2021). Higher executive control network coherence buffers against puberty-related increases in internalizing symptoms during the COVID-19 pandemic. *Biological Psychiatry: Cognitive Neuroscience and Neuroimaging*, *6*(1), 79–88. https://doi.org/10.1016/j.bpsc.2020.08.010

Chahal, R., Weissman, D. G., Hallquist, M. N., Robins, R. W., Hastings, P. D., & Guyer, A. E. (2021). Neural connectivity biotypes: Associations with internalizing problems throughout adolescence. *Psychological Medicine*, *51*(16), 2835–2845. https://doi.org/10.1017/S003329172000149X

Chai, X. J., Castañón, A. N., Öngür, D., & Whitfield-Gabrieli, S. (2012). Anticorrelations in resting state networks without global signal regression. *NeuroImage*, *59*(2), 1420–1428. https://doi.org/10.1016/j.neuroimage.2011.08.048

Cui, J., Li, M., Wu, Y., Shen, Q., Yan, W., Zhang, S., Chen, M., & Zhou, J. (2024). Exploring the mediating role of the ventral attention network and somatosensory motor network in the association between childhood trauma and depressive symptoms in major depressive disorders. *Journal of Affective Disorders*, *365*, 1–8. https://doi.org/10.1016/j.jad.2024.08.024

de Ross, R. L., Gullone, E., & Chorpita, B. F. (2002). The revised child anxiety and depression scale: A psychometric investigation with Australian youth. *Behaviour Change*, *19*(2), 90–101. https://doi.org/10.1375/bech.19.2.90

Essau, C. A. (2003). Comorbidity of anxiety disorders in adolescents. *Depression and Anxiety*, *18*(1), 1–6. https://doi.org/10.1002/da.10107

Essau, C. A. (2008). Comorbidity of depressive disorders among adolescents in community and clinical settings. *Psychiatry Research*, *158*(1), 35–42. https://doi.org/10.1016/j.psychres.2007.09.007

Feczko, E., Conan, G., Marek, S., Tervo-Clemmens, B., Cordova, M., Doyle, O., Earl, E., Perrone, A., Sturgeon, D., Klein, R., Harman, G., Kilamovich, D., Hermosillo, R., Miranda-Dominguez, O., Adebimpe, A., Bertolero, M., Cieslak, M., Covitz, S., Hendrickson, T., … Fair, D. A. (2021). Adolescent Brain Cognitive Development (ABCD) Community MRI Collection and Utilities. *bioRxiv*. https://doi.org/10.1101/2021.07.09.451638

Finn, E. S., Shen, X., Scheinost, D., Rosenberg, M. D., Huang, J., Chun, M. M., Papademetris, X., & Constable, R. T. (2015). Functional connectome fingerprinting: Identifying individuals using patterns of brain connectivity. *Nature Neuroscience*, *18*(11), Article 11. https://doi.org/10.1038/nn.4135

Fischl, B., Salat, D. H., Busa, E., Albert, M., Dieterich, M., Haselgrove, C., van der Kouwe, A., Killiany, R., Kennedy, D., Klaveness, S., Montillo, A., Makris, N., Rosen, B., & Dale, A. M. (2002). Whole brain segmentation: Automated labeling of neuroanatomical structures in the human brain. *Neuron*, *33*(3), 341–355. https://doi.org/10.1016/S0896-6273(02)00569-X

Garavan, H., Bartsch, H., Conway, K., Decastro, A., Goldstein, R. Z., Heeringa, S., Jernigan, T., Potter, A., Thompson, W., & Zahs, D. (2018). Recruiting the ABCD sample: Design considerations and procedures. *Developmental Cognitive Neuroscience*, *32*, 16–22. https://doi.org/10.1016/j.dcn.2018.04.004

Glasser, M. F., Sotiropoulos, S. N., Wilson, J. A., Coalson, T. S., Fischl, B., Andersson, J. L., Xu, J., Jbabdi, S., Webster, M., Polimeni, J. R., Van Essen, D. C., Jenkinson, M., & WU-Minn HCP Consortium. (2013). The minimal preprocessing pipelines for the Human Connectome Project. *NeuroImage*, *80*, 105–124. https://doi.org/10.1016/j.neuroimage.2013.04.127

Gogtay, N., Giedd, J. N., Lusk, L., Hayashi, K. M., Greenstein, D., Vaituzis, A. C., Nugent, T. F., Herman, D. H., Clasen, L. S., Toga, A. W., Rapoport, J. L., & Thompson, P. M. (2004). Dynamic mapping of human cortical development during childhood through early adulthood. *Proceedings of the National Academy of Sciences of the United States of America*, *101*(21), 8174–8179. https://doi.org/10.1073/pnas.0402680101

Goldstein-Piekarski, A. N., Ball, T. M., Samara, Z., Staveland, B. R., Keller, A. S., Fleming, S. L., Grisanzio, K. A., Holt-Gosselin, B., Stetz, P., Ma, J., & Williams, L. M. (2022). Mapping neural circuit biotypes to symptoms and behavioral dimensions of depression and anxiety. *Biological Psychiatry*, *91*(6), 561–571. https://doi.org/10.1016/j.biopsych.2021.06.024

Gordon, E. M., Chauvin, R. J., Van, A. N., Rajesh, A., Nielsen, A., Newbold, D. J., Lynch, C. J., Seider, N. A.,

Krimmel, S. R., Scheidter, K. M., Monk, J., Miller, R. L., Metoki, A., Montez, D. F., Zheng, A., Elbau, I., Madison, T., Nishino, T., Myers, M. J., … Dosenbach, N. U. F. (2023). A somato-cognitive action network alternates with effector regions in motor cortex. *Nature*, *617*(7960), 351–359. https://doi.org/10.1038/s41586-023-05964-2

Gordon, E. M., Laumann, T. O., Adeyemo, B., Huckins, J. F., Kelley, W. M., & Petersen, S. E. (2016). Generation and evaluation of a cortical area parcellation from resting-state correlations. *Cerebral Cortex*, *26*(1), 288–303. https://doi.org/10.1093/cercor/bhu239

Gracia-Tabuenca, Z., Barbeau, E. B., Xia, Y., & Chai, X. (2024). Predicting depression risk in early adolescence via multimodal brain imaging. *NeuroImage: Clinical*, *42*, 103604. https://doi.org/10.1016/j.nicl.2024.103604

Greene, A. S., Gao, S., Scheinost, D., & Constable, R. T. (2018). Task-induced brain state manipulation improves prediction of individual traits. *Nature Communications*, *9*(1), Article 1. https://doi.org/10.1038/s41467-018-04920-3

He, L., Wei, D., Yang, F., Zhang, J., Cheng, W., Feng, J., Yang, W., Zhuang, K., Chen, Q., Ren, Z., Li, Y., Wang, X., Mao, Y., Chen, Z., Liao, M., Cui, H., Li, C., He, Q., Lei, X., … Qiu, J. (2021). Functional Connectome Prediction of Anxiety Related to the COVID-19 Pandemic. *American Journal of Psychiatry*, *178*(6), 530–540. https://doi.org/10.1176/appi.ajp.2020.20070979

Ho, T. C., Shah, R., Mishra, J., May, A. C., & Tapert, S. F. (2022). Multi-level predictors of depression symptoms in the Adolescent Brain Cognitive Development (ABCD) study. *Journal of Child Psychology and Psychiatry*, *63*(12), 1523–1533. https://doi.org/10.1111/jcpp.13608

Hubbard, N. A., Bauer, C. C. C., Siless, V., Auerbach, R. P., Elam, J. S., Frosch, I. R., Henin, A., Hofmann, S. G., Hodge, M. R., Jones, R., Lenzini, P., Lo, N., Park, A. T., Pizzagalli, D. A., Vaz-DeSouza, F., Gabrieli, J. D. E., Whitfield-Gabrieli, S., Yendiki, A., & Ghosh, S. S. (2024). The Human Connectome Project of adolescent anxiety and depression dataset. *Scientific Data*, *11*(1), 837. https://doi.org/10.1038/s41597-024-03629-x

Hubbard, N. A., Siless, V., Frosch, I. R., Goncalves, M., Lo, N., Wang, J., Bauer, C. C. C., Conroy, K., Cosby, E., Hay, A., Jones, R., Pinaire, M., Vaz De Souza, F., Vergara, G., Ghosh, S., Henin, A., Hirshfeld-Becker, D. R., Hofmann, S. G., Rosso, I. M., …Whitfield-Gabrieli, S. (2020). Brain function and clinical characterization in the Boston adolescent neuroimaging of depression and anxiety study. *NeuroImage: Clinical*, *27*, 102240. https://doi.org/10.1016/j.nicl.2020.102240

Jin, J., Van Snellenberg, J. X., Perlman, G., DeLorenzo, C., Klein, D. N., Kotov, R., & Mohanty, A. (2020). Intrinsic neural circuitry of depression in adolescent females. *Journal of Child Psychology and Psychiatry*, *61*(4), 480–491. https://doi.org/10.1111/jcpp.13123

Kaiser, R. H., Andrews-Hanna, J. R., Wager, T. D., & Pizzagalli, D. A. (2015). Large-scale network dysfunction in major depressive disorder: A meta-analysis of resting-state functional connectivity. *JAMA Psychiatry*, *72*(6), 603–611. https://doi.org/10.1001/jamapsychiatry.2015.0071

Kaufman, J., Birmaher, B., Brent, D., Rao, U., Flynn, C., Moreci, P., Williamson, D., & Ryan, N. (1997). Schedule for affective disorders and schizophrenia for school-age children-present and lifetime version (K-SADS-PL): Initial reliability and validity data. *Journal of the American Academy of Child & Adolescent Psychiatry*, *36*(7), 980–988. https://doi.org/10.1097/00004583-199707000-00021

Kessler, R. C., Avenevoli, S., McLaughlin, K. A., Green, J. G., Lakoma, M. D., Petukhova, M., Pine, D. S., Sampson, N. A., Zaslavsky, A. M., & Merikangas, K. R. (2012). Lifetime co-morbidity of DSM-IV disorders in the US National Comorbidity Survey Replication Adolescent Supplement (NCS-A). *Psychological Medicine*, *42*(9), 1997–2010. https://doi.org/10.1017/S0033291712000025

Kessler, R. C., Berglund, P., Demler, O., Jin, R., Merikangas, K. R., & Walters, E. E. (2005). Lifetime prevalence and age-of-onset distributions of DSM-IV disorders in the National Comorbidity Survey Replication. *Archives of General Psychiatry*, *62*(6), 593–602. https://doi.org/10.1001/archpsyc.62.6.593

Kucyi, A., Esterman, M., Capella, J., Green, A., Uchida, M., Biederman, J., Gabrieli, J. D. E., Valera, E. M., & Whitfield-Gabrieli, S. (2021). Prediction of stimulus-independent and task-unrelated thought from functional brain networks. *Nature Communications*, *12*(1), Article 1. https://doi.org/10.1038/s41467-021-22027-0

Liu, J., Xu, P., Zhang, J., Jiang, N., Li, X., & Luo, Y. (2019). Ventral attention-network effective connectivity predicts individual differences in adolescent depression. *Journal of Affective Disorders*, *252*, 55–59. https://doi.org/10.1016/j.jad.2019.04.033

Lynch, C. J., Elbau, I. G., Ng, T., Ayaz, A., Zhu, S., Wolk, D., Manfredi, N., Johnson, M., Chang, M., Chou, J., Summerville, I., Ho, C., Lueckel, M., Bukhari, H., Buchanan, D., Victoria, L. W., Solomonov, N., Goldwaser, E., Moia, S., … Liston, C. (2024). Frontostriatal salience network expansion in individuals in depression. *Nature*, *633*(8030), 624–633. https://doi.org/10.1038/s41586-024-07805-2

Macêdo, M. A., Sato, J. R., Bressan, R. A., & Pan, P. M. (2022). Adolescent depression and resting-state fMRI brain networks: A scoping review of longitudinal studies. *Brazilian Journal of Psychiatry*, *44*, 420–433. https://doi.org/10.47626/1516-4446-2021-2032

MacNamara, A., DiGangi, J., & Phan, K. L. (2016). Aberrant spontaneous and task-dependent functional connections in the anxious brain. *Biological Psychiatry: Cognitive Neuroscience and Neuroimaging*, *1*(3), 278–287. https://doi.org/10.1016/j.bpsc.2015.12.004

Marek, S., Tervo-Clemmens, B., Calabro, F. J., Montez, D. F., Kay, B. P., Hatoum, A. S., Donohue, M. R., Foran, W., Miller, R. L., Hendrickson, T. J., Malone, S. M., Kandala, S., Feczko, E., Miranda-Dominguez, O., Graham, A. M., Earl, E. A., Perrone, A. J., Cordova, M., Doyle, O., … Dosenbach, N. U. F. (2022). Reproducible brain-wide association studies require thousands of individuals. *Nature*, *603*(7902), 654–660. https://doi.org/10.1038/s41586-022-04492-9

Mayberg, H. S., Lozano, A. M., Voon, V., McNeely, H. E., Seminowicz, D., Hamani, C., Schwalb, J. M., & Kennedy, S. H. (2005). Deep brain stimulation for treatment-resistant depression. *Neuron*, *45*(5), 651–660. https://doi.org/10.1016/j.neuron.2005.02.014

Menon, V. (2011). Large-scale brain networks and psychopathology: A unifying triple network model. *Trends in Cognitive Sciences*, *15*(10), 483–506. https://doi.org/10.1016/j.tics.2011.08.003

Morfini, F., Whitfield-Gabrieli, S., & Nieto-Castañón, A. (2023). Functional connectivity MRI quality control procedures in CONN. *Frontiers in Neuroscience*, *17*, 1092125. https://doi.org/10.3389/fnins.2023.1092125

Poldrack, R. A., Huckins, G., & Varoquaux, G. (2020). Establishment of best practices for evidence for prediction: A review. *JAMA Psychiatry*, *77*(5), 534–540. https://doi.org/10.1001/jamapsychiatry.2019.3671

Rosenblatt, M., Tejavibulya, L., Jiang, R., Noble, S., & Scheinost, D. (2024). Data leakage inflates prediction performance in connectome-based machine learning models. *Nature Communications*, *15*(1), 1829. https://doi.org/10.1038/s41467-024-46150-w

Scheinost, D., Noble, S., Horien, C., Greene, A. S., Lake, E. MR., Salehi, M., Gao, S., Shen, X., O'Connor, D., Barron, D. S., Yip, S. W., Rosenberg, M. D., & Constable, R. T. (2019). Ten simple rules for predictive modeling of individual differences in neuroimaging. *NeuroImage*, *193*, 35–45. https://doi.org/10.1016/j.neuroimage.2019.02.057

Sheline, Y. I., Barch, D. M., Price, J. L., Rundle, M. M., Vaishnavi, S. N., Snyder, A. Z., Mintun, M. A., Wang, S., Coalson, R. S., & Raichle, M. E. (2009). The default mode network and self-referential processes in depression. *Proceedings of the National Academy of Sciences of the United States of America*, *106*(6), 1942–1947. https://doi.org/10.1073/pnas.0812686106

Shen, X., Finn, E. S., Scheinost, D., Rosenberg, M. D., Chun, M. M., Papademetris, X., & Constable, R. T. (2017). Using connectome-based predictive modeling to predict individual behavior from brain connectivity. *Nature Protocols*, *12*(3), Article 3. https://doi.org/10.1038/nprot.2016.178

Siddiqi, S. H., Taylor, S. F., Cooke, D., Pascual-Leone, A., George, M. S., & Fox, M. D. (2020). Distinct symptom-specific treatment targets for circuit-based neuromodulation. *The American Journal of Psychiatry*, *177*(5), 435–446. https://doi.org/10.1176/appi.ajp.2019.19090915

Siless, V., Hubbard, N. A., Jones, R., Wang, J., Lo, N., Bauer, C. C. C., Goncalves, M., Frosch, I., Norton, D., Vergara, G., Conroy, K., De Souza, F. V., Rosso, I. M., Wickham, A. H., Cosby, E. A., Pinaire, M., Hirshfeld-Becker, D., Pizzagalli, D. A., Henin, A., … Yendiki, A. (2020). Image acquisition and quality assurance in the Boston Adolescent Neuroimaging of Depression and Anxiety study. *NeuroImage: Clinical*, *26*, 102242. https://doi.org/10.1016/j.nicl.2020.102242

Streiner, D. L. (2001). Regression toward the mean: Its etiology, diagnosis, and treatment. *The Canadian Journal of Psychiatry*, *46*(1), 72–76. https://doi.org/10.1177/070674370104600111

Sydnor, V. J., Larsen, B., Seidlitz, J., Adebimpe, A., Alexander-Bloch, A. F., Bassett, D. S., Bertolero, M. A., Cieslak, M., Covitz, S., Fan, Y., Gur, R. E., Gur, R. C., Mackey, A. P., Moore, T. M., Roalf, D. R., Shinohara, R. T., & Satterthwaite, T. D. (2023). Intrinsic activity development unfolds along a sensorimotor–association cortical axis in youth. *Nature Neuroscience*, *26*(4), 638–649. https://doi.org/10.1038/s41593-023-01282-y

Sylvester, C. M., Barch, D. M., Corbetta, M., Power, J. D., Schlaggar, B. L., & Luby, J. L. (2013). Resting state functional connectivity of the ventral attention network in children with a history of depression or anxiety. *Journal of the American Academy of Child & Adolescent Psychiatry*, *52*(12), 1326.e5–1336.e5. https://doi.org/10.1016/j.jaac.2013.10.001

Taxali, A., Angstadt, M., Rutherford, S., & Sripada, C. (2021). Boost in test–retest reliability in resting state fMRI with predictive modeling. *Cerebral Cortex*, *31*(6), 2822–2833. https://doi.org/10.1093/cercor/bhaa390

Toenders, Y. J., van Velzen, L. S., Heideman, I. Z., Harrison, B. J., Davey, C. G., & Schmaal, L. (2019). Neuroimaging predictors of onset and course of depression in childhood and adolescence: A systematic review of longitudinal studies. *Developmental Cognitive Neuroscience*, *39*, 100700. https://doi.org/10.1016/j.dcn.2019.100700

Tse, N. Y., Ratheesh, A., Tian, Y. E., Connolly, C. G., Davey, C. G., Ganesan, S., Gotlib, I. H., Harrison, B. J., Han, L. K. M., Ho, T. C., Jamieson, A. J., Kirshenbaum, J. S., Liu, Y., Ma, X., Ojha, A., Qiu, J., Sacchet, M. D., Schmaal, L., Simmons, A. N., … Zalesky, A. (2024). A mega-analysis of functional connectivity and network abnormalities in youth depression. *Nature Mental Health*, *2*(10), 1169–1182. https://doi.org/10.1038/s44220-024-00309-y

Uddin, L. Q., Betzel, R. F., Cohen, J. R., Damoiseaux, J. S., De Brigard, F., Eickhoff, S. B., Fornito, A., Gratton, C., Gordon, E. M., Laird, A. R., Larson-Prior, L., McIntosh, A. R., Nickerson, L. D., Pessoa, L., Pinho, A. L., Poldrack, R. A., Razi, A., Sadaghiani, S., Shine, J. M., … Spreng, R. N. (2023). Controversies and progress on standardization of large-scale brain network nomenclature. *Network Neuroscience*, *7*(3), 864–905. https://doi.org/10.1162/netn_a_00323

Uddin, L. Q., Castellanos, F. X., & Menon, V. (2025). Resting state functional brain connectivity in child and adolescent psychiatry: Where are we now? *Neuropsychopharmacology*, *50*(1), 196–200. https://doi.org/10.1038/s41386-024-01888-1

van Tol, M. J., van der Wee, N. J. A., & Veltman, D. J. (2021). Fifteen years of NESDA Neuroimaging: An overview of results related to clinical profile and bio-social risk factors of major depressive disorder and common anxiety disorders. *Journal of Affective Disorders*, *289*, 31–45. https://doi.org/10.1016/j.jad.2021.04.009

Westlin, C., Theriault, J. E., Katsumi, Y., Nieto-Castanon, A., Kucyi, A., Ruf, S. F., Brown, S. M., Pavel, M., Erdogmus, D., Brooks, D. H., Quigley, K. S., Whitfield-Gabrieli, S., & Barrett, L. F. (2023). Improving the study of brain-behavior relationships by revisiting basic assumptions. *Trends in Cognitive Sciences*, *27*(3), 246–257. https://doi.org/10.1016/j.tics.2022.12.015

Whitfield-Gabrieli, S., Wendelken, C., Nieto-Castañón, A., Bailey, S. K., Anteraper, S. A., Lee, Y. J., Chai, X., Hirshfeld-Becker, D. R., Biederman, J., Cutting, L. E., & Bunge, S. A. (2020). Association of intrinsic brain architecture with changes in attentional and mood symptoms during development. *JAMA Psychiatry*, *77*(4), 378–386. https://doi.org/10.1001/jamapsychiatry.2019.4208

Woo, C.-W., Chang, L. J., Lindquist, M. A., & Wager, T. D. (2017). Building better biomarkers: Brain models in translational neuroimaging. *Nature Neuroscience*, *20*(3), Article 3. https://doi.org/10.1038/nn.4478

Xu, J., Van Dam, N. T., Feng, C., Luo, Y., Ai, H., Gu, R., & Xu, P. (2019). Anxious brain networks: A coordinate-based activation likelihood estimation meta-analysis of resting-state functional connectivity studies in anxiety. *Neuroscience and Biobehavioral Reviews*, *96*, 21–30. https://doi.org/10.1016/j.neubiorev.2018.11.005

Yeo, T. B. T., Krienen, F. M., Sepulcre, J., Sabuncu, M. R., Lashkari, D., Hollinshead, M., Roffman, J. L., Smoller, J. W., Zöllei, L., Polimeni, J. R., Fischl, B., Liu, H., & Buckner, R. L. (2011). The organization of the human cerebral cortex estimated by intrinsic functional connectivity. *Journal of Neurophysiology*, *106*(3), 1125–1165. https://doi.org/10.1152/jn.00338.2011

Yu, R., & Chen, L. (2015). The need to control for regression to the mean in social psychology studies. *Frontiers in Psychology*, *5*, 1574. https://doi.org/10.3389/fpsyg.2014.01574

Zhang, J., Raya, J., Morfini, F., Urban, Z., Pagliaccio, D., Yendiki, A., Auerbach, R. P., Bauer, C. C. C., & Whitfield-Gabrieli, S. (2023). Reducing default mode network connectivity with mindfulness-based fMRI neurofeedback: A pilot study among adolescents with affective disorder history. *Molecular Psychiatry*, *28*(6), 2540–2548. https://doi.org/10.1038/s41380-023-02032-z

Supplementary Information

Brain functional connectivity predicts depression and anxiety during childhood and adolescence: A connectome-based predictive modeling approach

Francesca Morfini, MS[1,*], Aaron Kucyi, PhD[2], Jiahe Zhang, PhD[1,3], Clemens C. C. Bauer, PhD[1,3,4], Paul A. Bloom, PhD[5,6], David Pagliaccio, PhD[5,6], Nicholas A. Hubbard, PhD[7], Isabelle M. Rosso, PhD[8,9], Anastasia Yendiki, PhD[10], Satrajit S. Ghosh, PhD[4], Diego A. Pizzagalli, PhD[8,9], John D.E. Gabrieli, PhD[4], Susan Whitfield-Gabrieli, PhD[1,3,4,10], & Randy P. Auerbach, PhD, ABPP[5,6]

[1]Department of Psychology, Northeastern University, Boston, MA, USA
[2]Department of Psychological and Brain Sciences, Drexel University, Philadelphia, PA, USA
[3]Center for Precision Psychiatry, Massachusetts General Hospital, Boston, MA, USA
[4]Department of Brain and Cognitive Sciences and McGovern Institute for Brain Research, Massachusetts Institute of Technology, Cambridge, MA, USA
[5]Department of Psychiatry, Columbia University, New York, NY, USA
[6]Division of Child and Adolescent Psychiatry, New York State Psychiatric Institute, Columbia University, New York, NY, USA
[7]Department of Psychology, University of Nebraska-Lincoln, Lincoln, NE, USA
[8]Center for Depression, Anxiety, and Stress Research, McLean Hospital, Belmont, MA, USA
[9]Department of Psychiatry, Harvard Medical School, Boston, MA, USA
[10]Athinoula A. Martinos Center for Biomedical Imaging, Massachusetts General Hospital, Charlestown, MA, USA

DOI: https://doi.org/10.1162/IMAG.a.145

* Correspondence: Francesca Morfini, Department of Psychology, Center for Cognitive and Brain Health, Northeastern University, 805 Columbus Avenue, Boston, MA 02120, United States; Email: f.morfini.work@gmail.com

Table of Contents

Appendix S1. ABCD dataset description.

Appendix S2. ABCD MRI data preprocessing.

Appendix S3. BANDA dataset description.

Appendix S4. BANDA MRI data preprocessing.

Appendix S5. Mapping of Gordon parcellation to Yeo 7 canonical brain networks.

Appendix S6. Brain functional networks relative contribution to symptoms prediction.

Table S1. Participants, clinical, and scanner characteristics of the ABCD children.

Table S2. Participants, clinical, and scanner characteristics of the BANDA adolescents.

Table S3. BANDA clinical characteristics.

Table S4. RCADS subscales pairwise correlations in adolescents from BANDA.

Figure S1. CONSORT diagram of included and excluded participants.

Figure S2. Symptom severity and in-scanner head mean motion correlation.

Figure S3. Internal validation and predictions specificity in ABCD.

Figure S4. External validation and predictions specificity from ABCD to BANDA.

Figure S5. fMRI quality control distributions in BANDA.

Figure S6. Gordon parcellation assignment to Yeo 7 canonical networks.

Figure S7. Absolute network-network counts of the Symptoms Network.

Figure S8. Within-participant between-connections mean functional connectivity of the subcortical-to-cortical connections of the Symptoms Network in BANDA.

Supplementary References

Appendix S1. ABCD dataset description.

Sample characteristics and study design

ABCD is a public and longitudinal study from 21 USA sites aimed at characterizing neural, cognitive, and behavioral development in a large population (N = 11,875) of children of diverse race, ethnicity, education, environmental, and income levels who are 9-10-years-old at baseline. Each site received Institutional Review Board approval from their institution and written informed consent and assent were received by the guardian and participating children. Recruitment of children and their guardians was carried out through schools and community settings. A description of the recruitment, inclusion, and exclusion criteria, and study design has been detailed elsewhere (Garavan et al., 2018).

In this study, we included data from the baseline and 1-year follow-up visits. At each study visit, the MRI and clinical assessments typically happened on the same day. Anatomical and functional MRI data underwent a live quality control during data acquisition by scan operators, as well as both automated and visual inspection, including detection of excessive in-scanner head motion, signal to noise inhomogeneities, and anatomical abnormalities (Chai et al., 2012). Reasons for participant exclusion included in-scanner high motion, talking, falling asleep, using the safety squeeze ball to communicate with the operator, or interrupted scanning, and these reasons were coded into a pass or fail information. At both baseline and 1-year follow-up assessments, a guardian reported on their child's depression and anxiety severity using the Child Behavior Checklist (CBCL) Anxious/Depressed subscale (Achenbach, 1991).

We used data from the ABCD-BIDS Community Collection (**Figure S1A)**. This collection processed and analyzed only data from ABCD which had passed the quality control carried out by the consortia (excluded 2,471 participants). Additionally, we excluded participants

with missing CBCL Anxious/Depressed subscale *t*-transformed scores at either the baseline ($CBCL_{base}$) or 1-year follow-up ($CBCL_{y1}$) assessment (excluded additional 515 participants). We also excluded one of the family members of families that were scanned at different sites (of 10 families we excluded 5 participants, selecting the family member scanned at the site that had the biggest sample size out of the two sites). Lastly, exclusion criteria included having high an in-scanner mean head motion (FD > 0.25 mm) and less than 10 minutes of overall fMRI data after removing outliers. Overall, 3,718 participants were included in our study.

Depression and anxiety symptoms assessment

The Child Behavior Checklist (CBCL; Achenbach, 1991) is a 118-item caregiver report of child behavioral characteristics based on a 3-point Likert scale between 0 (*not true*) and 2 (*very true*). The subscale of interest was the Anxious/Depressed subscale based on 13 items with a range of possible scores between 0 and 26. Higher scores indicate greater symptom severity. The *t*-transformed scores were used. The Cronbach's alpha for our sample was 0.825 with a 95% confidence interval (CI) of [0.816, 0.833] at baseline and 0.818 with 95% CI [0.809, 0.826] at the 1-year assessment.

MRI data

MRI data were acquired at 3T via Siemens, General Electric, and Philips MRI scanners (**Table S1**) using multiband echo planar imaging (EPI) acquisition. MRI sequences were harmonized across scanners types and across sites, which had been in turn built starting from the Human Connectome Project (HCP) sequences (Smith et al., 2013). Imaging data characteristics are detailed elsewhere (Casey et al., 2018). Briefly, anatomical MRI data were T1-weighted multi-

echo magnetization-prepared rapid gradient echo (MPRAGE). Resting-state fMRI (rs-fMRI) data were four 5-min runs during which participants were instructed to passively gaze at a cross hair. The anatomical scans were acquired first, followed by the rs-fMRI runs.

Appendix S2. ABCD MRI data preprocessing.

Baseline rs-fMRI data were accessed from the ABCD-BIDS Community Collection 3165 (Feczko et al., 2021) as fully preprocessed, quality-controlled, data in the form of connectomes. Preprocessing details can be found under the Collection's online documentation (https://collection3165.readthedocs.io/en/stable/pipeline/). Briefly, the data had been processed using a modified version of the HCP pipeline (Glasser et al., 2013) customized and applied by the DCAN Lab (Feczko et al., 2021). Rs-fMRI data were registered onto the Montreal Neurological Institute (MNI) standard space using a combination of surface and volume coordinate systems. Preprocessed rs-fMRI data were then further denoised by removing signal factors, including head motion, mean time series for white matter, cerebrospinal fluid, and global signal, as well as movement factors such as realignment parameters. All frames with framewise displacement (FD) < 0.2 mm (Chai et al., 2012) were retained and used for functional connectivity estimation.

Preprocessed data were parcellated following a cortical (Gordon et al., 2016) and subcortical (Fischl et al., 2002) schema, band-pass filtered (0.008, 0.09 Hz), and concatenated. Then, the time series of each parcel were extracted, and Pearson's correlated to the time series of every other parcel, and Fisher r-to-z-transformed. This process resulted in the construction of one symmetrical 352-by-352 connectivity matrix (i.e. connectome) per participant, representing their whole-brain functional connectivity patterns (**Figure 1** from the main text).

Appendix S3. BANDA dataset description.

Sample characteristics and study design

Information of the study protocol and information of the full sample for the Boston Adolescent Neuroimaging of Depression and Anxiety (BANDA) dataset, also referred to as Human Connectomes Project for Disease related to Anxiety and Depression in Adolescents, are described elsewhere (Hubbard et al., 2020, 2024; Siless et al., 2020). Briefly, participants were included if ages between 14 and 17 years-old at the baseline assessment and both participant and their guardian were fluent in English. Exclusion criteria for the participants were: unable to undergo MRI scanning, presenting with IQ < 85, having any neurodevelopmental disorders, bipolar disorder, psychotic disorder, premature birth, serious medication conditions, history of serious head injury, or hospitalization following a neurological or cardiovascular disease.

Clinical assignment included the Kiddie Schedule for Affective Disorders and Schizophrenia Present and Lifetime Version (K-SADS; Kaufman et al., 1997) adapted to provide DSM-5 compatible classifications. Depressed-anxious participants were defined as those presenting at baseline with a primary diagnosis of at least one depressive (i.e., major depressive disorder, dysthymia, or depression not otherwise specified) and/or anxiety disorders (i.e., generalized anxiety disorder, social phobia, separation anxiety, panic disorder, agoraphobia, or specific phobia). Presenting with a diagnosis of attention-deficit/hyperactivity disorder (ADHD), which is highly comorbid with depression and anxiety, and/or being on psychotropic medications were not considered exclusion criteria for the depressed-anxious group (for further rationale see Hubbard et al., 2020, 2024). Healthy controls were defined as those without any lifetime history of psychiatric disorders at baseline.

All adolescents included in the current study participated in at least two study visits, one year apart. The baseline visit included an MRI scanning session, a diagnostic interview, collection of self-report, collection of parental measures of symptom severity including the Revised Child Anxiety and Depression Scale (RCADS; de Ross et al., 2002), and neurocognitive assessments. During the 1-year follow-up assessment, symptom severity was assessed again. As part of the full protocol for the BANDA study (Hubbard et al., 2020, 2024), a number of other measures of psychopathology, cognitive performance, and general demographic information were acquired at both baseline and 1-year follow-up assessments via the following: Behavioral Inhibition and Behavioral Activation Questionnaire (BISBAS; Carver & White, 1994), Chapman Handedness Inventory (Chapman & Chapman, 1987), Columbia Suicide Severity Rating Scale (CSSRS; Posner et al., 2011), Mood and Feelings Questionnaire (MFQ; Angold et al., 1995), Risky Behavior Questionnaire for Adolescents (RBQA; Auerbach & Gardiner, 2012), Snaith-Hamilton Pleasure Scale (SHAPS; Carver & White, 1994), State-Trait Anxiety Inventory (STAI; Spielberger et al., 1970), Wechsler Abbreviated Scale of Intelligence (WASI-II; Wechsler, 2018), in addition to the RCADS.

In this study, participants were excluded if there were incomplete data consisting of baseline anatomical, rs-fMRI data, or completion of the RCADS at both the baseline ($RCADS_{base}$) and 1-year assessment ($RCADS_{y1}$). Participants were excluded also if the in-scanner mean head motion was FD > 0.25 mm. The final sample included 150 adolescents (see **Table S2** for the sample's demographic and clinical information; **Figure S1B** for a flowchart of the included and excluded participants).

Depression and anxiety symptom assessment

Depression and anxiety severity was assessed with the Revised Child Anxiety and Depression Scale (RCADS; de Ross et al., 2002). The RCADS total scores were calculated as the sum of the 47 items rated on a 4-point Likert scale between 0 (*never*) and 3 (*always*) and represented depression and anxiety severity. RCADS total scores can range between 0 and 141, with higher scores representing greater symptom severity. The RCADS includes the following subscales: social phobia, panic disorder, major depression, separation anxiety, generalized anxiety, and obsessive-compulsive disorder. A measure of self-reported anxiety severity can be calculated by summing all the subscales except for the major depression subscale. The *t*-transformed scores were used. The Cronbach's alpha for the RCADS total scores of our sample was 0.970 with 95% CI [0.964, 0.977] at baseline and 0.963 with 95% CI [0.954, 0.971] at the 1-year assessment.

MRI data

The description of MRI sequences, protocols, and harmonization with other HCP datasets are more extensively reported elsewhere (Siless et al., 2020; Tozzi et al., 2020). Briefly, the MRI data were collected on a Siemens 3T Prisma MRI with a 64-channel head coil. One high resolution anatomical image was acquired with a T1-weighted MPRAGE sequence (0.8 mm isotropic voxels, field of view = 256 x 240 x 167 mm, TR = 2,400 ms, TE = 2.18 ms). rs-fMRI were acquired using simultaneous multi-slice (2.0 mm isotropic voxels, 72 slices, multiband acceleration factor = 8, TR = 800 ms, TE = 37 ms, flip angle = 52°), each consisting of 420 volumes lasting 5 min and 46 s. Two sets of two eyes-open rs-fMRI (four total runs lasting overall ~23) with opposite phase encoding (PE) direction (Anterior-Posterior [AP] and Posterior-

Anterior [PA]) were acquired and were alternated with the acquisition of a Spin-Echo fieldmap with opposite PE direction (AP-PA).

Appendix S4. BANDA MRI data preprocessing.

BANDA connectomes generation

After preprocessing and denoising, anatomical and functional data were parcellated, denoised, and organized into connectomes using the CONN Toolbox (Whitfield-Gabrieli & Nieto-Castanon, 2012). FMRI data were parcellated into 333 cortical (Gordon et al., 2016) and 19 subcortical regions (Fischl et al., 2002). Connectomes were generated by calculating the Fisher-z transform of the Pearson *r* correlation coefficient between the mean time series of each of the 352 regions to the time series of every other region. This step resulted in one, symmetrical connectome per participant and mimicked the connectome constructions carried out for the ABCD participants.

Appendix S5. Mapping of Gordon parcellation to Yeo 7 canonical brain networks.

For interpretation purposes, each of the regions from the Gordon parcellation was mapped onto one of the 7 Yeo networks (Yeo et al., 2011) by calculating the spatial overlap of each parcel to the Yeo's networks liberal masks, both in MNI volume space, using the CONN v.21a (Whitfield-Gabrieli & Nieto-Castanon, 2012) in-built conn_roioverlaps function. Briefly, each voxel forming a parcel would be assigned to one Yeo network. The Yeo network with the highest count of voxels in a parcel and a total match count of at least 50 voxels would define which network that parcel would be assigned to. Five of the 333 Gordon's parcels were not assigned to any of Yeo's networks (voxels overlap = 19.40 ± 23.90, range [1, 48]).

Appendix S6. Brain functional networks relative contribution to symptoms prediction.

To characterize the relative contribution of each canonical network pair to the prediction of prospective symptom severity, we calculated counts of connections of all within- and between-networks pairs from the Symptoms Network and normalized them by their total possible size (Greene et al., 2018), as follows:

$$\text{Contribution score}_{AB} = \frac{\frac{Surviving\ Edges_{AB}}{Surviving\ Edges_{total}}}{\frac{Edges_{AB}}{Edges_{total}}}$$

where A and B represent two canonical networks; $Surviving\ Edges_{AB}$ / $Surviving\ Edges_{total}$ represents the ratio between the surviving connections between two canonical networks (A and B) over all the surviving connections (n = 251 unique connections)); and the denominator $Edges_{AB}$ / $Edges_{total}$ represents the ratio between all possible connections between network A and network B over all possible connections of the chosen parcellation, i.e., [352 * (352 -1)] / 2 = 61,776 connections . Contribution scores above 1 identify canonical network pairs that are overrepresented in our Symptoms Network relative to their possible size.

Table S1. Participants, clinical, and scanner characteristics of the ABCD children.

ABCD dataset	Included participants (n = 3,718)
Sex [n, %]	
Male	1,967 (52.90%)
Female	1,751 (47.10%)
Race [n]	
White	3,136
Black or African American	494
Asian	264
American Indian Native American	123
Hawaiian or Pacific Islander	23
Others	171
Unknown or not reported	24
Ethnicity [n]	
Not Hispanic or Latino	3,074
Hispanic or Latino	606
Do not know, refuse to answer, NA	38
Age (months) [n]	
Baseline	120.16 (±7.49)
1-Year Follow-Up	132.33 (±7.7)
CBCL Anxious/Depressed raw score	
Baseline	2.54 (±3.12)
1-Year follow-up	2.59 (±3.1)
CBCL Anxious/Depressed *t*-score	
Baseline	53.48 (±6.06)
1-Year follow-up	53.51 (±6.02)
Scanner manufacturer [n]	
SIEMENS	2,640
General Electric Medical Systems	832
Philips Medical Systems	246
Scanner Model [n]	
Prisma	1,359
Prisma_fit	1,281
DISCOVERY MR750	793
Achieva dStream	149
Ingenia	97
SIGNA Creator	39
In-scanner mean motion (mm)	0.16 (±0.05)

Characteristics are presented for the participants included in our study (n = 3,718). Values are reported as mean (± standard deviation), unless otherwise specified. ABCD: Adolescent Brain Cognitive Development; CBCL: Child Behavior Checklist.

Table S2. Participants, clinical, and scanner characteristics of the BANDA adolescents.

BANDA dataset	Healthy (n = 54)	Depressed-Anxious (n = 96)	t|χ2	p
Sex [n]			0.84	0.36
Female	30	62		
Male	24	34		
Age (months)				
Baseline	182.94 (±9.91)	186.62 (±10.43)	-2.11	0.04 *
1-Year follow-up	195,85 (±10.26)	199.8 (±10.43)	-2.24	0.03 *
Race [n]			1.31	0.93
White	43	77		
More than one race	7	14		
Asian	2	2		
Black or African American	1	1		
Hawaiian or Pacific Islander	0	1		
Unknown or not reported	1	1		
Ethnicity [n]			1.14	0.57
Not Hispanic or Latino	50	87		
Hispanic or Latino	4	7		
Unknown or not reported	0	2		
RCADS total raw score				
Baseline	14.17 (±9.46)	50.26 (±24.13)	-10.53	<0.001 ***
1-Year follow-up	15.46 (±12.08)	39.53 (±21.45)	-7.59	<0.001 ***
RCADS total *t*-score				
Baseline	36.04 (±4.43)	56.47 (±14.26)	-10.24	<0.001 ***
1-Year follow-up	36.7 (±5.25)	49.07 (±11.5)	-7.47	<0.001 ***
In-scanner mean motion (mm)	0.1 (±0.04)	0.1 (±0.04)	-0.21	0.83

Characteristics are presented for the participants included in our study (n = 150). Values are reported as mean (± standard deviation), unless otherwise specified. The depressed-anxious group includes participants presenting at baseline with at least a primary depressive and/or anxiety disorder diagnosis, whereas healthy participants had no current or lifetime history of DSM-5 mental disorders at the baseline assessment. Comparisons between the depressed-anxious and healthy participants represent either statistics from independent-sample t-test or Chi square test. BANDA: Boston Adolescent Neuroimaging of Depression and Anxiety; RCADS: Revised Child Depression and Anxiety Scale; *: $p < 0.05$; ***: $p < 0.001$.

Table S3. BANDA clinical characteristics.

Depressed-Anxious BANDA participants	Baseline (n = 96)	1-Year Follow-Up (n = 71)
DSM-5 depressive disorders		
Major depressive disorder	38	18
Dysthymia	2	5
Depression not otherwise specified	0	0
DSM-5 anxiety disorders		
Generalized anxiety disorder	51	35
Social phobia	46	39
Separation anxiety	6	1
Panic disorder	11	8
Agoraphobia	5	2
Specific phobia	23	16
DSM-5 other disorders		
Attention-deficit/hyperactivity disorder	27	20
Obsessive-compulsive or related disorders	11	8
Post-traumatic stress disorder	2	0

Presence of diagnoses reported in the table were based on the Kiddie Schedule for Affective Disorders and Schizophrenia Present and Lifetime Version (Kaufman et al., 1997) clinical interview adapted to assess DSM-5 (American Psychiatric Association, 2013) mental disorders. The table reports current diagnoses at each study assessment. DSM-5: Diagnostic and Statistical Manual of Mental Disorders 5th edition.

Table S4. RCADS subscales pairwise correlations in adolescents from BANDA.

		Baseline			1-year follow-up		
Subscale1	**Subscale2**	**r**	**CI 95%**	**p-corrected**	**r**	**CI 95%**	**p-corrected**
Total	Social phobia	0.8753	[0.83 0.91]	<0.0001	0.8859	[0.85 0.92]	<0.0001
Total	Panic disorder	0.8977	[0.86 0.92]	<0.0001	0.8368	[0.78 0.88]	<0.0001
Total	MDD	0.8953	[0.86 0.92]	<0.0001	0.8942	[0.86 0.92]	<0.0001
Total	GAD	0.9091	[0.88 0.93]	<0.0001	0.8901	[0.85 0.92]	<0.0001
Total	OCD	0.7669	[0.69 0.83]	<0.0001	0.6647	[0.56 0.75]	<0.0001
Total	SAD	0.7899	[0.72 0.84]	<0.0001	0.7796	[0.71 0.84]	<0.0001
Total	Total anxiety	0.9895	[0.99 0.99]	<0.0001	0.9856	[0.98 0.99]	<0.0001
Social phobia	Panic	0.7205	[0.63 0.79]	<0.0001	0.6865	[0.59 0.76]	<0.0001
Social phobia	MDD	0.7053	[0.61 0.78]	<0.0001	0.7208	[0.63 0.79]	<0.0001
Social phobia	GAD	0.7558	[0.68 0.82]	<0.0001	0.7612	[0.68 0.82]	<0.0001
Social phobia	OCD	0.5663	[0.45 0.67]	<0.0001	0.4332	[0.29 0.55]	<0.0001
Social phobia	SAD	0.6061	[0.49 0.70]	<0.0001	0.6251	[0.52 0.71]	<0.0001
Social phobia	Total anxiety	0.8914	[0.85 0.92]	<0.0001	0.9001	[0.86 0.93]	<0.0001
Panic disorder	MDD	0.7552	[0.68 0.82]	<0.0001	0.7394	[0.66 0.80]	<0.0001
Panic disorder	GAD	0.7777	[0.71 0.83]	<0.0001	0.6494	[0.55 0.73]	<0.0001
Panic disorder	OCD	0.6334	[0.53 0.72]	<0.0001	0.4199	[0.28 0.54]	<0.0001
Panic disorder	SAD	0.7023	[0.61 0.78]	<0.0001	0.5746	[0.46 0.67]	<0.0001
Panic disorder	Total anxiety	0.904	[0.87 0.93]	<0.0001	0.8281	[0.77 0.87]	<0.0001
MDD	GAD	0.7786	[0.71 0.83]	<0.0001	0.7298	[0.64 0.80]	<0.0001
MDD	OCD	0.6596	[0.56 0.74]	<0.0001	0.5137	[0.39 0.62]	<0.0001
MDD	SAD	0.6346	[0.53 0.72]	<0.0001	0.5815	[0.46 0.68]	<0.0001
MDD	Total anxiety	0.8215	[0.76 0.87]	<0.0001	0.8058	[0.74 0.86]	<0.0001
GAD	OCD	0.7191	[0.63 0.79]	<0.0001	0.6598	[0.56 0.74]	<0.0001
GAD	SAD	0.7154	[0.63 0.79]	<0.0001	0.7383	[0.66 0.80]	<0.0001
GAD	Total anxiety	0.911	[0.88 0.93]	<0.0001	0.9023	[0.87 0.93]	<0.0001
OCD	SAD	0.5645	[0.44 0.66]	<0.0001	0.6327	[0.53 0.72]	<0.0001
OCD	Total anxiety	0.7676	[0.69 0.83]	<0.0001	0.6855	[0.59 0.76]	<0.0001
SAD	Total anxiety	0.8051	[0.74 0.86]	<0.0001	0.812	[0.75 0.86]	<0.0001

Pairwise Pearson correlations among Revised Child Anxiety and Depression Scale (RCADS) subscales at the baseline and 1-year follow-up assessments for the BANDA adolescents (n = 150). RCADS subscales included generalized anxiety (GAD), major depressive disorder (MDD), obsessive-compulsive disorder (OCD), panic disorder, separation anxiety disorder (SAD), and social phobia. Total Anxiety reflects the sum of all subscales except for MDD, whereas Total includes all subscales. *P* values are two-sided and Bonferroni-corrected for multiple comparisons.

Figure S1. CONSORT diagram of included and excluded participants.

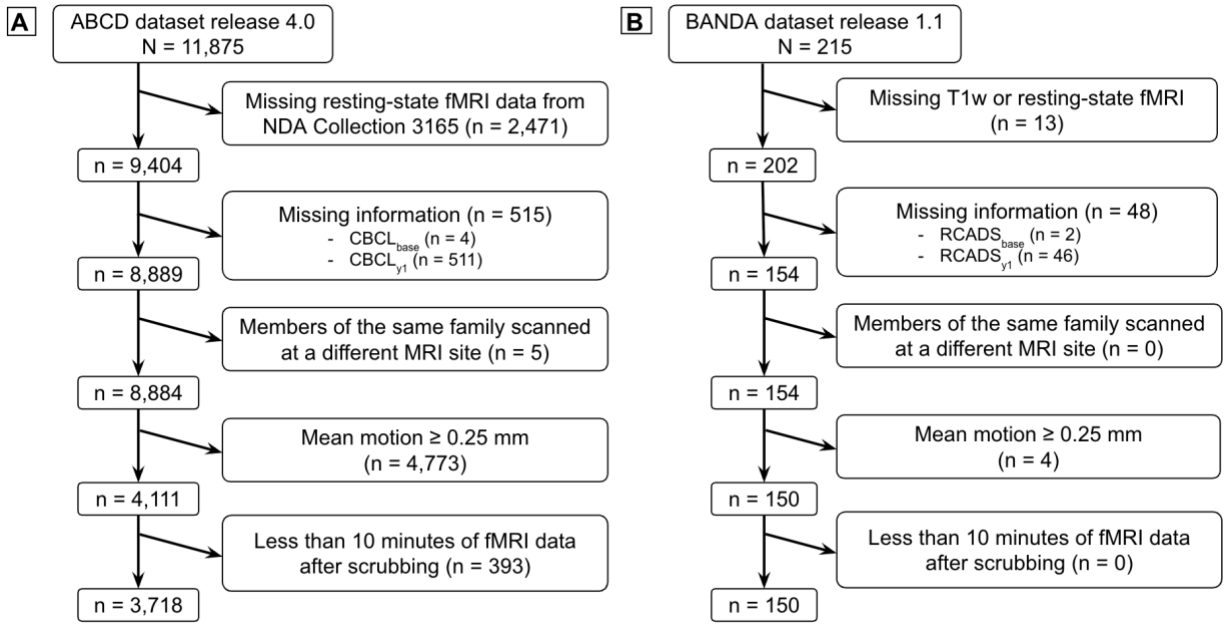

(**A**) Flow of exclusion for ABCD participants. rs-fMRI data were obtained from the fully preprocessed ABCD-BIDS Community Collection 3165 (Feczko et al., 2021) which only included data from the Annual Curated ABCD 4.0 Data Release (Barch et al., 2018) that had passed the Data Analysis Imaging Center quality control (Chai et al., 2012). (**B**) Flow of exclusion for BANDA participants. ABCD: Adolescent Brain Cognitive Development Study; BANDA: Boston Adolescent Neuroimaging of Depression and Anxiety; CBCL: Child Behavior Checklist, Anxious/Depressed subscale raw scores; fMRI: functional magnetic resonance imaging; NDA: National Institute of Mental Health Data Archive; RCADS: Revised Child Depression and Anxiety Scale, total raw scores.

Figure S2. Symptom severity and in-scanner head mean motion correlation.

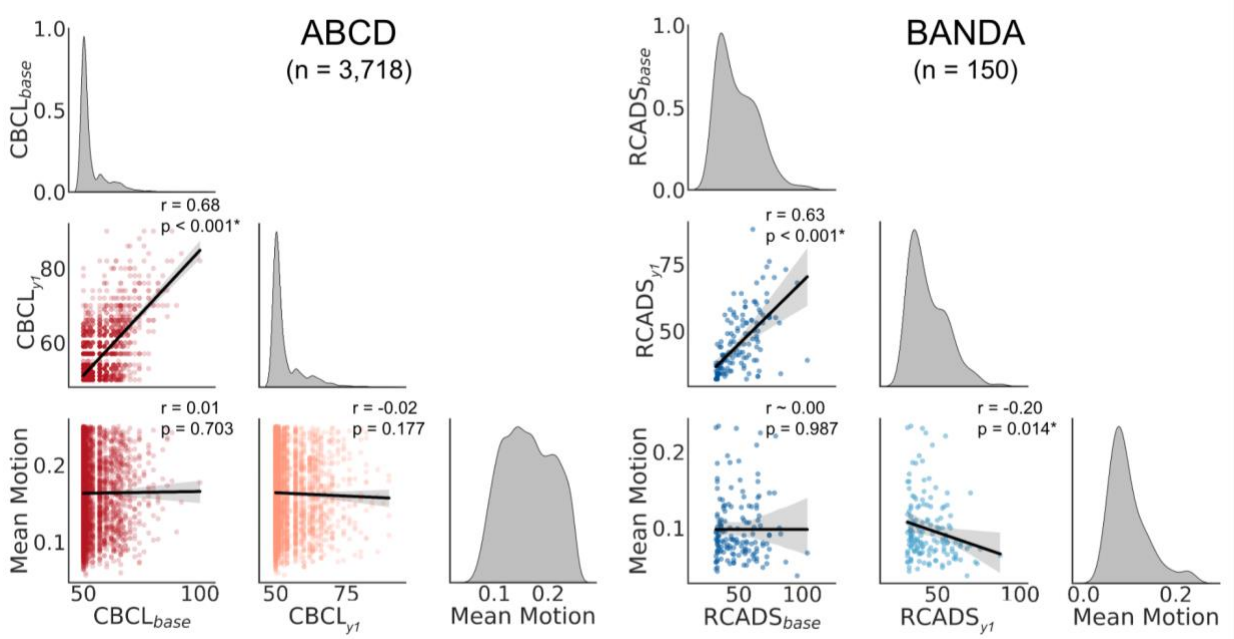

The scatterplots represent Pearson's correlations coefficients *r* between depression and anxiety symptom severity at the baseline and 1-year follow-up assessments with in-scanner head mean motion (framewise displacement in mm Chai et al., 2012) for the included participants of the ABCD (left) and BANDA cohorts (right). Symptom severity was calculated using the CBCL Anxious/Depressed subscale *t*-transformed scores in ABCD and using the RCADS *t*-transformed total scores in BANDA, respectively. The plots report the 99% confidence interval (shaded areas). ABCD: Adolescent Brain Cognitive Development Study; BANDA: Boston Adolescent Neuroimaging of Depression and Anxiety; base: baseline assessment; CBCL: Child Behavior Checklist Anxious/Depressed subscale, *t*-transformed scores; CPM: connectome-based predictive modeling; y1: 1-year follow-up assessment; RCADS: Revised Child Depression and Anxiety Scale, *t*-transformed total scores. *: $p < 0.001$.

Figure S3. Internal validation and predictions specificity in ABC

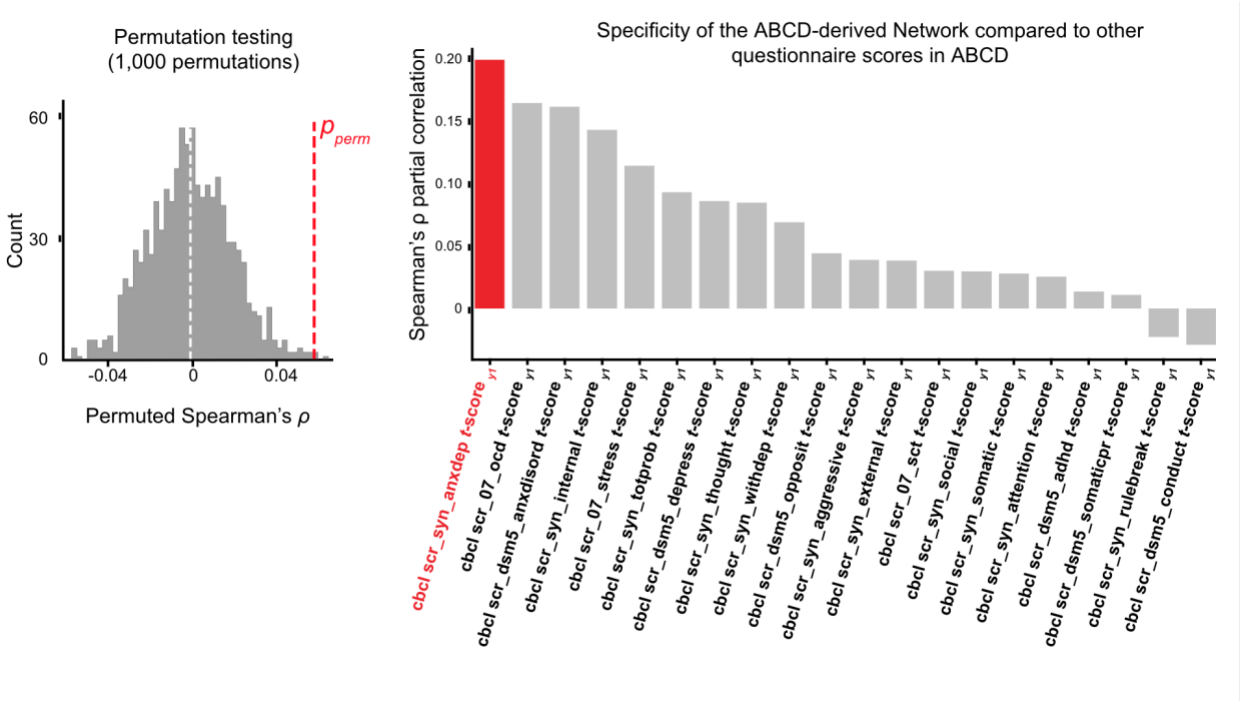

(**Left**) Null distribution of ρ values generated from 1,000 permutations derived with shuffled data (i.e., connectivity values of one participant were used to predict the symptom severity of another random participant). The permuted distribution is centered around $\rho = 0$ (white dashed line). Negative ρ values represent cases where the predictions were inaccurate, for example mild symptoms were predicted but severe symptoms were observed. Network significance (p_{perm}, red dashed line) was defined as the proportion of permuted ρ values larger than the ρ value (average of 100 iterations) generated by the observed data (Shen et al., 2017). (**Right**) To evaluate the specificity of the Symptoms Network to anxiety and depression in the ABCD children, we computed Spearman's partial correlation with each of all CBCL subscales as outcome (adjusting for baseline $CBCL_{base}$, sex, age, and mean head motion). Note, the results shown here differ from those reported in the main text (e.g., for $CBCL_{y1}$, red bar), in that here we use the Networks Symptoms to extract network strengths from participants, we use Spearman's partial correlation and not cross-validation and permutation testing, and we used the full sample (n = 3,718). Consequently, the bar graph does not represent predictions, rather in-sample correlations. Nonetheless, the correlation estimates for the different CBCL subscales offer a comparison between the performance of Symptoms Network for anxiety and depression as compared to other symptoms.

Figure S4. External validation and predictions specificity from ABCD to BANDA.

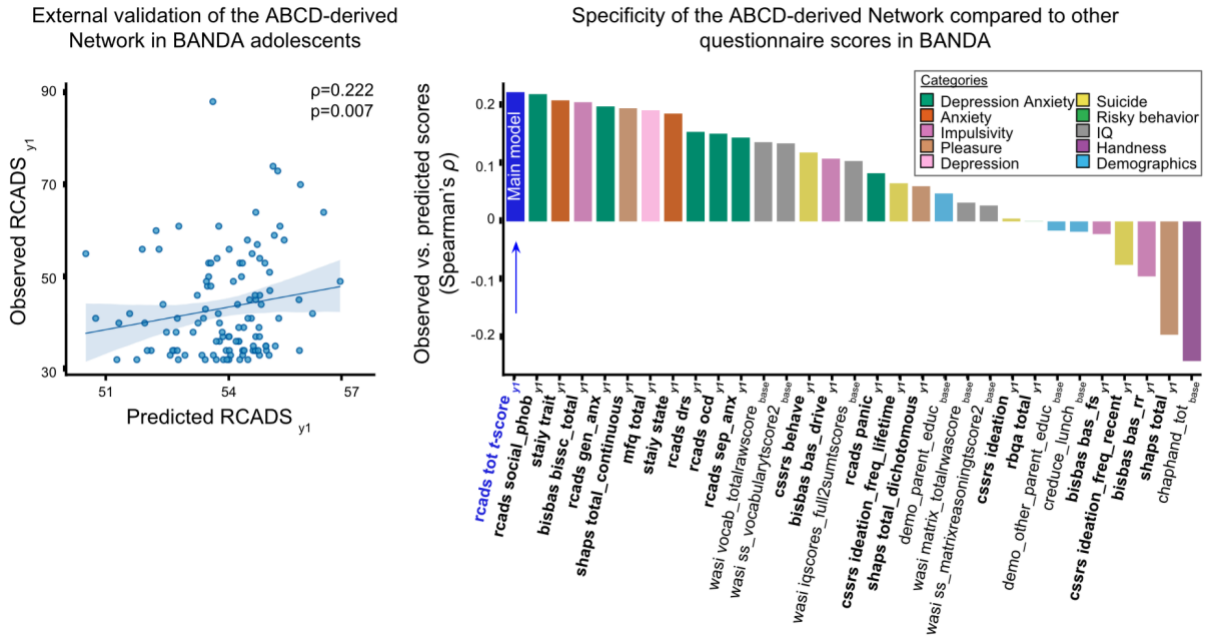

(**Left**) Observed vs. predicted $RCADS_{y1}$ scores in BANDA adolescents (n = 150). Predicted $RCADS_{y1}$ scores were generated from functional connectivity based on the ABCD-derived Symptoms Network. The generalizability of the Symptoms Network from ABCD to BANDA was assessed using Spearman's rank correlation to minimize the impact of symptom scores skewness (Spearman's $r = 0.222$, $p = 0.007$). The fitted trend line and 95% CI are shown for visualization purposes (Pearson's $r = 0.210$, $p = 0.011$). (**Right**) To assess the specificity of the Symptoms Network to internalizing symptoms (rather than to a more general vulnerability to psychopathology), the Symptoms Network was used to predict a range of self-reported measures in BANDA at the 1-year follow-up, including internalizing psychopathology, other psychopathology, cognitive measures, and general demographic measures. The barplot displays the Spearman's ρ correlation coefficients (y-axis) of the main model presented in the manuscript (i.e., $RCADS_{y1}$; blue bar, the first bar on the left) as it compares to all other measures (x-axis) acquired at the 1-year follow-up assessment and a few demographic measures acquired at baseline. Every model was corrected for $RCADS_{base}$, sex at birth, age, and mean head motion. Measures included the BIS-BAS (Carver & White, 1994) drive, reward responsiveness, and fun seeking subscales; Chapman Handedness Inventory (Chapman & Chapman, 1987), CSSRS (Posner et al., 2011), MFQ (Angold et al., 1995), RBQA (Auerbach & Gardiner, 2012); SHAPS (Carver & White, 1994), STAI (Spielberger et al., 1970), and WASI-II (Wechsler, 2018). BISBAS: Behavioral Inhibition and Behavioral Activation Questionnaire; CSSRS: Columbia Suicide Severity Rating Scale; y1: 1-year follow-up assessment; MFQ: Mood and Feelings Questionnaire; STAI: State-Trait Anxiety Inventory; RBQA: Risky Behavior Questionnaire for Adolescents; RCADS: Revised Child Anxiety and Depression Scale; SHAPS: Snaith-Hamilton Pleasure Scale; WASI-II: Wechsler Abbreviated Scale of Intelligence.

Figure S5. fMRI quality control distributions in BANDA.

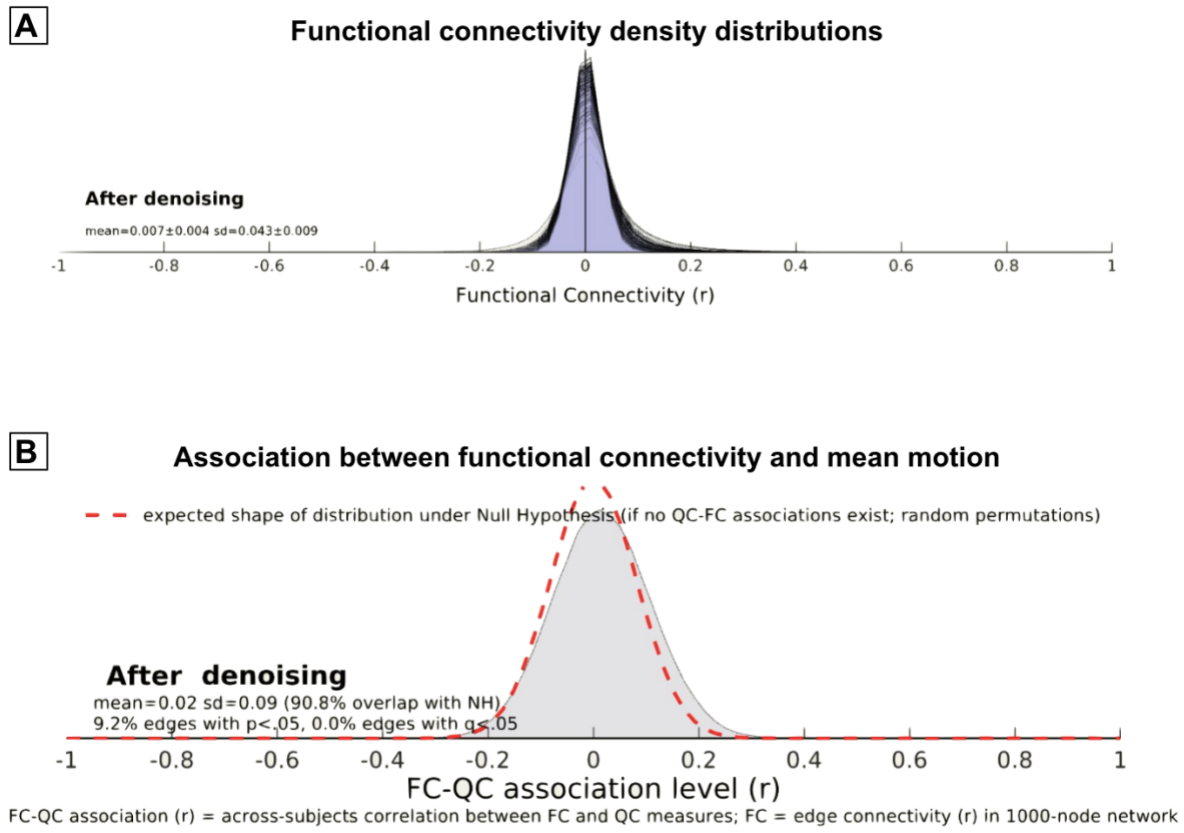

(**A**) Density distributions of functional connectivity strengths (*r* coefficients) after denoising between 1,000 randomly selected voxels for each participant (BANDA n = 150). (**B**) QC-FC correlation distribution between functional connectivity estimates and in-scanner mean head motion. The red dotted line represents a theoretical artifact-free null-hypothesis distribution (Morfini et al., 2023). Higher levels of overlap between the QC-FC distribution and the red dotted line (e.g., above 95%) can be considered indicative of negligible modulations in the connectivity correlation structure driven by a source of noise. FC: functional connectivity; NH: null hypothesis; QC: quality control.

Figure S6. Gordon parcellation assignment to Yeo 7 canonical networks.

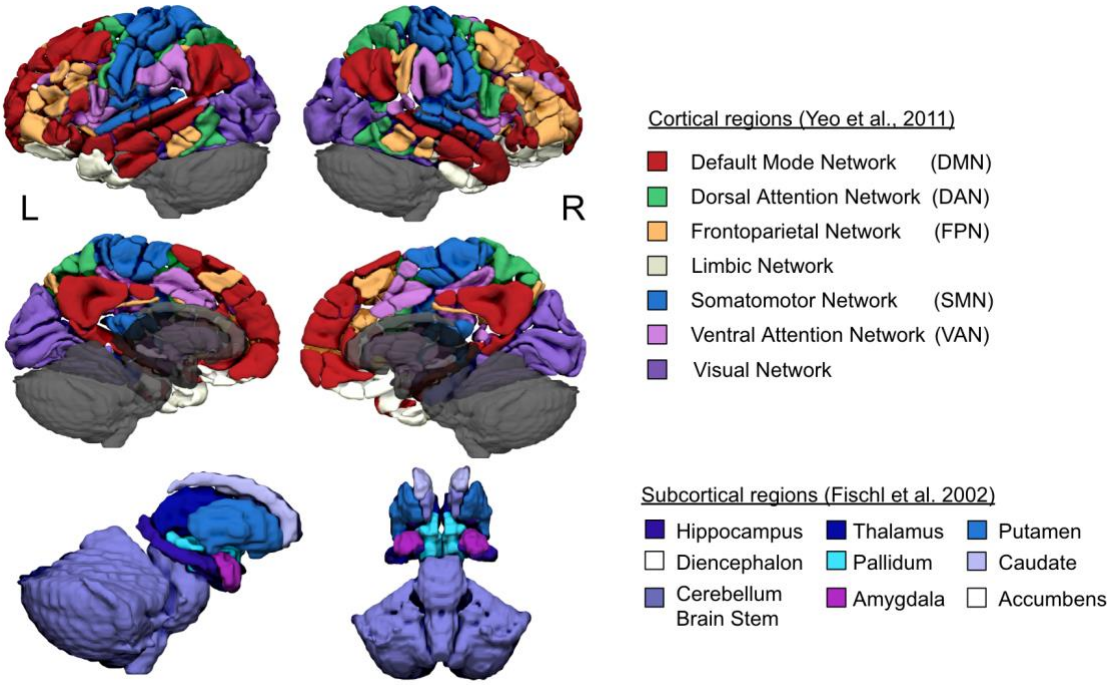

The brain images represent the 333 cortical Gordon parcels (Gordon et al., 2016) and the 19 subcortical parcels from the Freesurfer Atlas (Fischl et al., 2002) color-coded following the assignment to the canonical networks defined by Yeo and colleagues (Yeo et al., 2011).

Figure S7. Absolute network-network counts of the Symptoms Network.

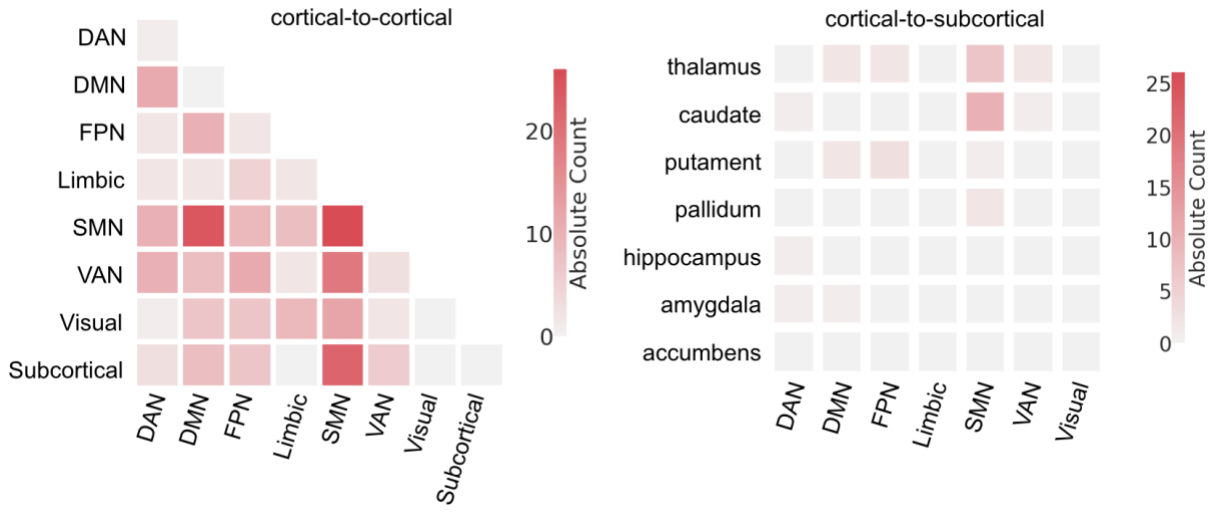

Absolute counts of the connections from the Symptoms Network. Counts are reported for cortical-to-cortical (**left**) and cortical-to-subcortical connections (**right**). DAN: Dorsal Attention Network; DMN: Default Mode Network; FPN: Frontoparietal Network; VAN: Ventral Attention Network; SMN: Somatomotor Network.

Figure S8. Within-participant between-connections mean functional connectivity of the subcortical-to-cortical connections of the Symptoms Network in BANDA.

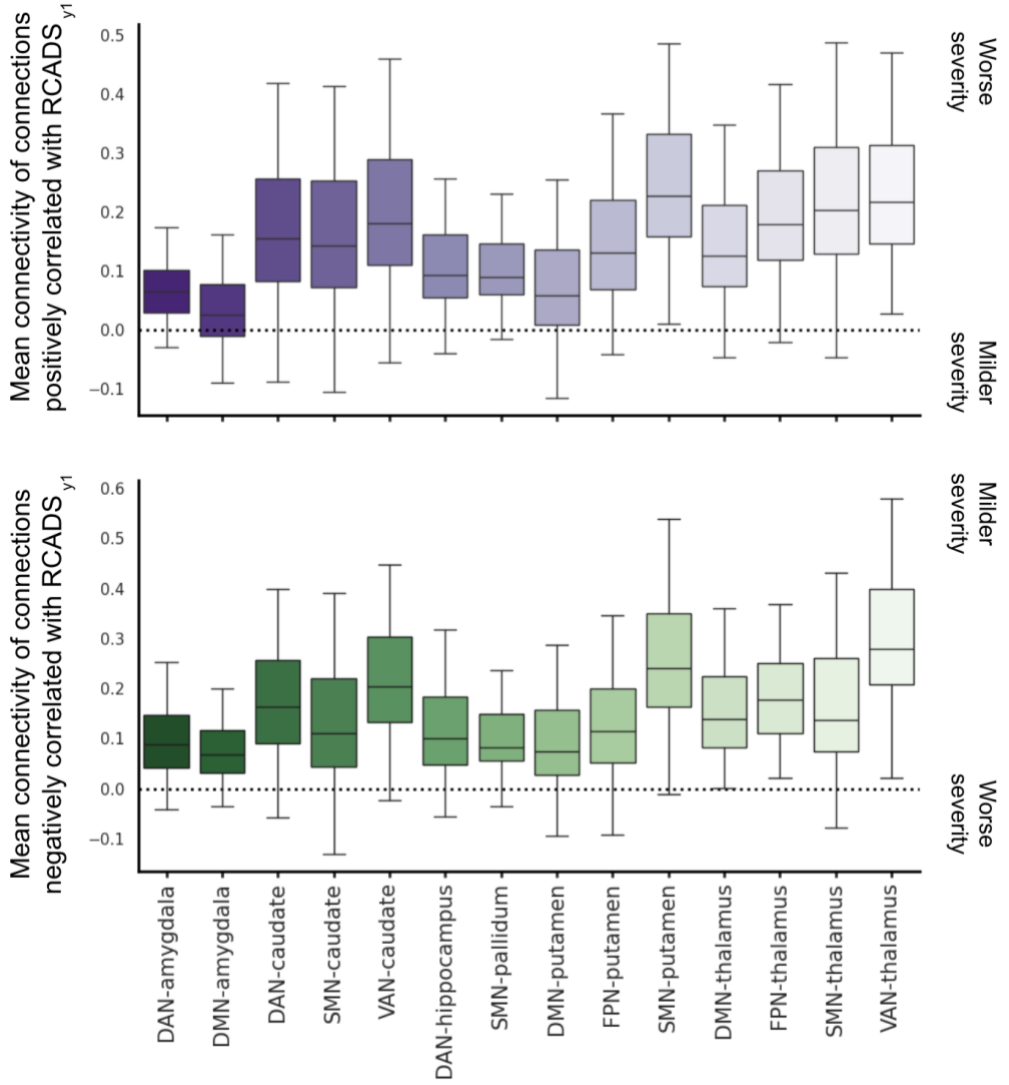

The plots represent the distributions of within-participant between-connection mean functional connectivity for every overrepresented subcortical-to-cortical-network pair of the Symptoms Network. For example, for every participant separately, we calculated the mean functional connectivity for all connections of a specific subcortical-to-cortical network pair. Each boxplot represents the distribution of the mean functional connectivity for a subset of connections for the included (n = 150) BANDA adolescents. To aid results interpretation, connections were split into a set of connections positively (purple, top) or negatively (green, bottom) correlated with $RCADS_{y1}$. For example, higher mean connectivity values in the boxplot for DAN-amygdala were correlated with worse $RCADS_{y1}$ severity in the positive connections (first purple boxplot) but were correlated with milder $RCADS_{y1}$ severity in the (first green boxplot). DAN: Dorsal Attention Network; DMN: Default Mode Network; FPN: Frontoparietal Network; SMN: Somatomotor Network; VAN: Ventral Attention Network.

Supplementary References

Achenbach, T. M. (1991). *Manual for the Child Behavior Checklist/4-18 and 1991 Profile*. Department of Psychiatry, University of Vermont.

American Psychiatric Association. (2013). *Diagnostic and statistical manual of mental disorders: DSM-5™, 5th ed* (pp. xliv, 947). American Psychiatric Publishing, Inc. https://doi.org/10.1176/appi.books.9780890425596

Angold, A., Costello, E. J., Messer, S. C., & Pickles, A. (1995). Development of a short questionnaire for use in epidemiological studies of depression in children and adolescents. *International Journal of Methods in Psychiatric Research*, *5*(4), 237–249.

Auerbach, R. P., & Gardiner, C. K. (2012). Moving beyond the trait conceptualization of self-esteem: The prospective effect of impulsiveness, coping, and risky behavior engagement. *Behaviour Research and Therapy*, *50*(10), 596–603. https://doi.org/10.1016/j.brat.2012.06.002

Barch, D. M., Albaugh, M. D., Avenevoli, S., Chang, L., Clark, D. B., Glantz, M. D., Hudziak, J. J., Jernigan, T. L., Tapert, S. F., Yurgelun-Todd, D., Alia-Klein, N., Potter, A. S., Paulus, M. P., Prouty, D., Zucker, R. A., & Sher, K. J. (2018). Demographic, physical and mental health assessments in the adolescent brain and cognitive development study: Rationale and description. *Developmental Cognitive Neuroscience*, *32*, 55–66. https://doi.org/10.1016/j.dcn.2017.10.010

Carver, C. S., & White, T. L. (1994). Behavioral inhibition, behavioral activation, and affective responses to impending reward and punishment: The BIS/BAS Scales. *Journal of Personality and Social Psychology*, *67*(2), 319–333. https://doi.org/10.1037/0022-3514.67.2.319

Casey, B. J., Cannonier, T., Conley, M. I., Cohen, A. O., Barch, D. M., Heitzeg, M. M., Soules, M. E., Teslovich, T., Dellarco, D. V., Garavan, H., Orr, C. A., Wager, T. D., Banich, M. T., Speer, N. K., Sutherland, M. T., Riedel, M. C., Dick, A. S., Bjork, J. M., Thomas, K. M., … Dale, A. M. (2018). The Adolescent Brain Cognitive Development (ABCD) study: Imaging acquisition across 21 sites. *Developmental Cognitive Neuroscience*, *32*, 43–54. https://doi.org/10.1016/j.dcn.2018.03.001

Chai, X. J., Castañón, A. N., Öngür, D., & Whitfield-Gabrieli, S. (2012). Anticorrelations in resting state networks without global signal regression. *NeuroImage*, *59*(2), 1420–1428. https://doi.org/10.1016/j.neuroimage.2011.08.048

Chapman, L. J., & Chapman, J. P. (1987). The measurement of handedness. *Brain and Cognition*, *6*(2), 175–183. https://doi.org/10.1016/0278-2626(87)90118-7

de Ross, R. L., Gullone, E., & Chorpita, B. F. (2002). The Revised Child Anxiety and Depression Scale: A Psychometric Investigation with Australian Youth. *Behaviour Change*, *19*(2), 90–101. https://doi.org/10.1375/bech.19.2.90

Feczko, E., Conan, G., Marek, S., Tervo-Clemmens, B., Cordova, M., Doyle, O., Earl, E., Perrone, A., Sturgeon, D., Klein, R., Harman, G., Kilamovich, D., Hermosillo, R., Miranda-Dominguez, O., Adebimpe, A., Bertolero, M., Cieslak, M., Covitz, S., Hendrickson, T., … Fair, D. A. (2021). *Adolescent Brain Cognitive Development (ABCD) Community MRI Collection and Utilities* (p. 2021.07.09.451638). bioRxiv. https://doi.org/10.1101/2021.07.09.451638

Fischl, B., Salat, D. H., Busa, E., Albert, M., Dieterich, M., Haselgrove, C., van der Kouwe, A., Killiany, R., Kennedy, D., Klaveness, S., Montillo, A., Makris, N., Rosen, B., & Dale, A. M. (2002). Whole Brain Segmentation: Automated Labeling of Neuroanatomical

Structures in the Human Brain. *Neuron*, *33*(3), 341–355. https://doi.org/10.1016/S0896-6273(02)00569-X

Garavan, H., Bartsch, H., Conway, K., Decastro, A., Goldstein, R. Z., Heeringa, S., Jernigan, T., Potter, A., Thompson, W., & Zahs, D. (2018). Recruiting the ABCD sample: Design considerations and procedures. *Developmental Cognitive Neuroscience*, *32*, 16–22. https://doi.org/10.1016/j.dcn.2018.04.004

Glasser, M. F., Sotiropoulos, S. N., Wilson, J. A., Coalson, T. S., Fischl, B., Andersson, J. L., Xu, J., Jbabdi, S., Webster, M., Polimeni, J. R., Van Essen, D. C., Jenkinson, M., & WU-Minn HCP Consortium. (2013). The minimal preprocessing pipelines for the Human Connectome Project. *NeuroImage*, *80*, 105–124. https://doi.org/10.1016/j.neuroimage.2013.04.127

Gordon, E. M., Laumann, T. O., Adeyemo, B., Huckins, J. F., Kelley, W. M., & Petersen, S. E. (2016). Generation and Evaluation of a Cortical Area Parcellation from Resting-State Correlations. *Cerebral Cortex*, *26*(1), 288–303. https://doi.org/10.1093/cercor/bhu239

Greene, A. S., Gao, S., Scheinost, D., & Constable, R. T. (2018). Task-induced brain state manipulation improves prediction of individual traits. *Nature Communications*, *9*(1), Article 1. https://doi.org/10.1038/s41467-018-04920-3

Hubbard, N. A., Bauer, C. C. C., Siless, V., Auerbach, R. P., Elam, J. S., Frosch, I. R., Henin, A., Hofmann, S. G., Hodge, M. R., Jones, R., Lenzini, P., Lo, N., Park, A. T., Pizzagalli, D. A., Vaz-DeSouza, F., Gabrieli, J. D. E., Whitfield-Gabrieli, S., Yendiki, A., & Ghosh, S. S. (2024). The Human Connectome Project of adolescent anxiety and depression dataset. *Scientific Data*, *11*(1), 837. https://doi.org/10.1038/s41597-024-03629-x

Hubbard, N. A., Siless, V., Frosch, I. R., Goncalves, M., Lo, N., Wang, J., Bauer, C. C. C., Conroy, K., Cosby, E., Hay, A., Jones, R., Pinaire, M., Vaz De Souza, F., Vergara, G., Ghosh, S., Henin, A., Hirshfeld-Becker, D. R., Hofmann, S. G., Rosso, I. M., … Whitfield-Gabrieli, S. (2020). Brain function and clinical characterization in the Boston adolescent neuroimaging of depression and anxiety study. *NeuroImage: Clinical*, *27*, 102240. https://doi.org/10.1016/j.nicl.2020.102240

Kaufman, J., Birmaher, B., Brent, D., Rao, U., Flynn, C., Moreci, P., Williamson, D., & Ryan, N. (1997). Schedule for Affective Disorders and Schizophrenia for School-Age Children-Present and Lifetime Version (K-SADS-PL): Initial Reliability and Validity Data. *Journal of the American Academy of Child & Adolescent Psychiatry*, *36*(7), 980–988. https://doi.org/10.1097/00004583-199707000-00021

Morfini, F., Whitfield-Gabrieli, S., & Nieto-Castañón, A. (2023). Functional connectivity MRI quality control procedures in CONN. *Frontiers in Neuroscience*, *17*. https://www.frontiersin.org/articles/10.3389/fnins.2023.1092125

Posner, K., Brown, G. K., Stanley, B., Brent, D. A., Yershova, K. V., Oquendo, M. A., Currier, G. W., Melvin, G. A., Greenhill, L., Shen, S., & Mann, J. J. (2011). The Columbia–Suicide Severity Rating Scale: Initial Validity and Internal Consistency Findings From Three Multisite Studies With Adolescents and Adults. *American Journal of Psychiatry*, *168*(12), 1266–1277. https://doi.org/10.1176/appi.ajp.2011.10111704

Shen, X., Finn, E. S., Scheinost, D., Rosenberg, M. D., Chun, M. M., Papademetris, X., & Constable, R. T. (2017). Using connectome-based predictive modeling to predict individual behavior from brain connectivity. *Nature Protocols*, *12*(3), Article 3. https://doi.org/10.1038/nprot.2016.178

Siless, V., Hubbard, N. A., Jones, R., Wang, J., Lo, N., Bauer, C. C. C., Goncalves, M., Frosch,

I., Norton, D., Vergara, G., Conroy, K., De Souza, F. V., Rosso, I. M., Wickham, A. H., Cosby, E. A., Pinaire, M., Hirshfeld-Becker, D., Pizzagalli, D. A., Henin, A., … Yendiki, A. (2020). Image acquisition and quality assurance in the Boston Adolescent Neuroimaging of Depression and Anxiety study. *NeuroImage: Clinical*, *26*, 102242. https://doi.org/10.1016/j.nicl.2020.102242

Smith, S. M., Beckmann, C. F., Andersson, J., Auerbach, E. J., Bijsterbosch, J., Douaud, G., Duff, E., Feinberg, D. A., Griffanti, L., Harms, M. P., Kelly, M., Laumann, T., Miller, K. L., Moeller, S., Petersen, S., Power, J., Salimi-Khorshidi, G., Snyder, A. Z., Vu, A. T., … Glasser, M. F. (2013). Resting-state fMRI in the Human Connectome Project. *NeuroImage*, *80*, 144–168. https://doi.org/10.1016/j.neuroimage.2013.05.039

Spielberger, C., Gorsuch, R., & Luschene, E. (1970). *Manual For the State-Trait Anxiety Interview (Self-Evaluation Questionnaire)*. https://scholar.google.com/scholar_lookup?title=Manual%20For%20the%20State-Trait%20Anxiety%20Interview%20&publication_year=1970&author=C.D.%20Spielberger&author=R.L.%20Gorsuch&author=E.%20Luschene

Tozzi, L., Staveland, B., Holt-Gosselin, B., Chesnut, M., Chang, S. E., Choi, D., Shiner, M., Wu, H., Lerma-Usabiaga, G., Sporns, O., Barch, D. M., Gotlib, I. H., Hastie, T. J., Kerr, A. B., Poldrack, R. A., Wandell, B. A., Wintermark, M., & Williams, L. M. (2020). The human connectome project for disordered emotional states: Protocol and rationale for a research domain criteria study of brain connectivity in young adult anxiety and depression. *NeuroImage*, *214*, 116715. https://doi.org/10.1016/j.neuroimage.2020.116715

Wechsler, D. (2018). *Wechsler Abbreviated Scale of Intelligence—Second Edition* [Dataset]. https://doi.org/10.1037/t15171-000

Whitfield-Gabrieli, S., & Nieto-Castanon, A. (2012). *Conn: A Functional Connectivity Toolbox for Correlated and Anticorrelated Brain Networks | Brain Connectivity*. https://www.liebertpub.com/doi/abs/10.1089/brain.2012.0073

Yeo, T. B. T., Krienen, F. M., Sepulcre, J., Sabuncu, M. R., Lashkari, D., Hollinshead, M., Roffman, J. L., Smoller, J. W., Zöllei, L., Polimeni, J. R., Fischl, B., Liu, H., & Buckner, R. L. (2011). The organization of the human cerebral cortex estimated by intrinsic functional connectivity. *Journal of Neurophysiology*, *106*(3), 1125–1165. https://doi.org/10.1152/jn.00338.2011